University of New Orleans
ScholarWorks@UNO

University of New Orleans Theses and Dissertations | Dissertations and Theses

Spring 5-19-2017

Paleohydrology and Paleoecology of the Neogene Siwalik rocks, Nepalese Himalaya using multi-proxy lipid biomarker isotopic study

Prabhat Chandra Neupane
University of New Orleans, pcneupan@uno.edu

Follow this and additional works at: https://scholarworks.uno.edu/td

 Part of the Geology Commons

Recommended Citation

Neupane, Prabhat Chandra, "Paleohydrology and Paleoecology of the Neogene Siwalik rocks, Nepalese Himalaya using multi-proxy lipid biomarker isotopic study" (2017). *University of New Orleans Theses and Dissertations*. 2348.
https://scholarworks.uno.edu/td/2348

This Dissertation is protected by copyright and/or related rights. It has been brought to you by ScholarWorks@UNO with permission from the rights-holder(s). You are free to use this Dissertation in any way that is permitted by the copyright and related rights legislation that applies to your use. For other uses you need to obtain permission from the rights-holder(s) directly, unless additional rights are indicated by a Creative Commons license in the record and/or on the work itself.

This Dissertation has been accepted for inclusion in University of New Orleans Theses and Dissertations by an authorized administrator of ScholarWorks@UNO. For more information, please contact scholarworks@uno.edu.

Paleohydrology and Paleoecology of the Neogene Siwalik rocks, Nepalese Himalaya using multi-proxy lipid biomarker isotopic study

A Dissertation

Submitted to the Graduate Faculty of the
University of New Orleans
In partial fulfillment of the
Requirements for the degree of

Doctor of Philosophy
In
Engineering and applied Science
Earth and Environmental Sciences

By

Prabhat Chandra Neupane
B.Sc. Geology, Tribhuvan University, Nepal, 2001
M.Sc. Geology, Tribhuvan University, Nepal, 2004
M.S. in Geology, University of New Orleans, USA, 2011

May, 2017

Dedicated to my father Lila Nath Neupane and mother Tulashi Prabha Neupane.

ACKNOWLEDGEMENTS

I like to extend my sincere gratitude to my co-advisors Dr. M. Royhan Gani and Dr. Nahid D. Gani for giving me an opportunity to conduct the PhD research and encouraging me to grow as a research scientist. Specially, their advice and support on research are priceless. I like to thank Dr. Yongsong Huang and my committee members – Dr. Mark Kulp, Dr. Ioannis Georgiou and Dr. Bhaskar Kura – for their encouragement, insightful comments and valuable suggestions. I am also thankful to Pitambar Gautam, Erwin Appel and Wolfgang Rösler for kindly providing detailed paleomagnetic data for the Karnali River and Surai Khola sections. I am indebted to Prakash Ulak for providing detail information about the study area, Kabir Sharma and Ishwor Thapa for their assistance during fieldwork, Ghanashyam Neupane for suggestion during manuscript preparation, and Hiranya Sahoo for his guidance. Thanks are also due to Rafael Tarozo and Jiaju Zhao for their helps during geochemical analysis of samples at Brown University. I am thankful to University of New Orleans, Western Kentucky University, and Society for Sedimentary Geology (SEPM) for providing financial support for this research. I would like to express gratitude to all the faculty and staff (especially Dr. Martin O'Connel, Al Falster and Ms. Linda Miller) of the Department of Earth and Environmental Sciences for their direct and indirect help during my PhD study.

A special thanks to my family, especially to elder brother Krishna and sister-in-law. Finally, I would like to express my appreciation to my beloved wife Kabita for her continuous support in this educational journey and my two daughters Serene and Pristine who are the source of my positive energy and encouragement.

TABLE OF CONTENTS

LIST OF FIGURES

ABSTRACT

This study deploys compound-specific multi-proxy isotopic study of lipid biomarkers to understand Neogene climatic and ecological variabilities in the Himalayan foreland. The investigation of compound-specific carbon and hydrogen isotopes along with glycerol dialkyl glycerol tetraether (GDGT) is the first of its kind for the Nepalese Siwalik. A total of 49 mudstone (and some paleosol) samples were collected from the paleomagnetically age-constrained Siwalik strata in the Surai Khola and Karnali River sections.

$\delta^{13}C$ results suggest a domination of C_3 trees between 12 and 8.5 Ma, and a stepwise expansion of C_4 grasses starting gradually at 8.5 Ma and culminating rapidly around 5.5 Ma. δD results show an overall gradual increase in rainfall since 12 Ma, with a rapid intensification around 5.5 Ma. The negative correlation between rainfall and GDGT-derived paleotemperature prior to 5.5 Ma indicates that the region experienced higher rainfalls during colder periods and vice versa. We propose that this negative correlation could be related to the strong presence of mid-latitude westerlies in the region because of the subdued Himalayas, when summer monsoon winds were weaker, that brought enhanced winter-precipitation particularly during colder periods. After 5.5 Ma, our data show a conspicuous positive correlation between rainfall and annual temperature, indicating the onset of modern-style seasonality in rainfall in the Indian subcontinent, which generates more rainfall during summer than during winter. Notably, this initiation of the Indian monsoon around 5.5 Ma favored the dominance of C_4 grasses over C_3 trees that is reflected in our $\delta^{13}C$ data.

Key words: *Multi-proxy; lipid biomarkers; vegetation change, paleohydrology; monsoon; Neogene; Siwalik*

Chapter 1

Introduction

1.1 Motivation:

Late Neogene global expansion of C_4 grasses replacing C_3 trees is well document (Quade et al., 1989, 1995; Fox and Koch, 2004; Tipple and Pagani, 2010; Cerling et al., 2011). Although a drop in atmospheric $_pCO_2$ level was advocated as a likely mechanism for this vegetation shift (Cerling et al. 1993, 1997), recent studies have pointed to a number of other mechanisms including changes in precipitation intensity, seasonality, aridity, and fire frequency (Huang et al. 2007, Tipple and Pagani, 2007, Behrensmeyer et al. 2007, Stromberg, 2011).

To understand the mode and tempo of climate change in the Himalayan front (Siwalik), a number of extensive studies were conducted. These studies presented different and sometimes conflicting opinions on the vegetation shift (from C_3 to C_4), onset of South Asian monsoon, and phases of rainfall intensification (Quade et al., 1989, 1995; Quade and Cerling, 1995; Dettman et al., 2001; Gupta et al., 2004; Sanyal et al., 2010; Singh et al., 2012). Most of these studies agreed on the expansion of C_4 plants replacing C_3 vegetation and the monsoon intensification during the Neogene, but the mechanism and timing are still contentious. For a better understanding of the Neogene climate and vegetation change, we deploy the compound specific isotope analysis (CSIA) of $\delta^{13}C$ and δD, and glycerol dialkyle glycerol tetraether (GDGT) based paleotemperature study for the first time in the Nepalese Siwalik. In this study, we have chosen the Surai Khola and Karnali River sections for three main reasons. First, these sections have well exposed and accessible Neogene outcrops. Second, both sections are paleomagnetically age constrained (Appel et al., 1991; Gautam and Fujiwara, 2000). Third, in the Surai Khola section, Quade et al. (1995) already performed $\delta^{13}C$ and $\delta^{18}O$ studies based on the bulk isotope analysis,

which is an advantage to validate our new method of CSIA in the region. Similarly, the Karnali River section probably represents the oldest exposed Siwalik succession in Nepal.

1.2 defined problems

Although, the expansion of vegetation and phases of monsoon intensification are widely discussed in the Himalayan foreland, timing and mechanism of such changes are still debated and needed to investigate further. To understand the plausible causes and linkages of climate on vegetation, we aim to address the following problems:

1. Was the Neogene vegetation change synchronous along the Siwalik range and what was the mechanism of this vegetation shift?
2. When did the South Asian monsoon start? Did overall rainfall increase or decrease in the Himalaya during the Neogene?
3. Variability of Neogene temperature in the region, and its relation with the vegetation shift and rainfall intensification.

1.3 Approach

To bring a new insight on the Neogene climate change in the Nepalese Siwalik, several extensive fieldwork were carried out in the two river sections of Nepal. Mudstone and some paleosol samples were collected at a high resolution (0.25 -0.5 myr) interval from the paleomagnetically age-constrained Siwalik strata (Appel et al., 1991; Gautam and Fujiwara, 2000). The cutting edge technique of compound specific isotope analysis (CSIA) was performed to analyze sedimentary rock samples with sophisticated equipment such as: accelerated solvent extractor (ASE 200) to extract organic compounds from the samples, gas chromatograph and fame ionization detector (GC-FID) to determine the concentration of organic compounds in the

analyzed samples, and high performance liquid chromatography mass spectrometer (HPLC-MS) to obtain compound specific isotopic values of carbon and hydrogen. These analyses were conducted in the organic geochemistry lab of Brown University. We focused on three biomarker proxies ($\delta^{13}C$, δD and GDGT), and prepared two separate chapters as publishable standalone manuscripts.

Chapter two of this dissertation is focused on carbon isotope study ($\delta^{13}C$) to understand the vegetation changes from C_3 tress to C_4 grasses. We attempted to validate our CSIA $\delta^{13}C$ result by comparing with the previous bulk carbon isotope study in the Surai Khola section (Quade et al., 1995), and to establish new carbon isotope record for the first time in the Karnali River section. The carbon isotope study of the two river sections demonstrates an asynchronous expansion of C_4 vegetation even within a short lateral distance of about 200 km. In the Surai Khola section, the C_4 vegetation started to appear around 8.5 Ma and dominated around 5.5 Ma. However, in the Karnali River section, although some contribution of C_4 plants were observed between 14.5 to 9.5 Ma, no clear sign of C_4 plant expansion was observed untill 5.2 Ma, Which is the age of our youngest sample.

In chapter three, we bring all the multiproxy ($\delta^{13}C$, δD and GDGTs) data together to understand the relationship between the climate and vegetation change in the region. The result of δD and GDGT-derived paleotemperature show a negative correlation before 5.5 Ma in both river sections, suggesting a lack of seasonality, when more rainfall occurred during colder periods and vice versa. After 5.5 Ma, climate reversed with a synchronous increase in both rainfall and temperature. We suggest that the modern-style Indian monsoon started around 5.5 Ma, favoring C_4 grasses over C_3 trees.

Chapter 2

Neogene vegetation shift in the Nepalese Siwalik: A compound specific isotopic study of lipid biomarkers

Abstract:

The late Neogene vegetation change of C_4 plants replacing C_3 plants is widely documented across the world. This vegetation shift has been particularly well documented in the Himalayan foreland based on $\delta^{13}C$ isotopic data from paleosol carbonates and bulk organic matter in the Siwalik sedimentary rocks of Pakistan, India and Nepal, showing asynchronous expansion of C_4 plants between 8 to ~5 Ma, 9 to 6 Ma, and around 7 Ma, respectively. In this study, we deploy compound-specific isotopic analysis of biomarkers extracted from shale and paleosols in the paleomagnetically age-constrained Nepalese Siwalik in the Surai Khola and Karnali River sections for a better understanding of this vegetation shift.

Our $\delta^{13}C$ *n*-alkane (C_{27-31}) results from the Surai Khola section suggest a C_3 plant domination between 12 and 8.5 Ma, and a stepwise expansion of C_4 plants starting gradually at 8.5 Ma and culminating rapidly at 5.2 Ma. However in the Karnali River section, where the age of our youngest sample is 5.2 Ma, data show no clear sign of C_4 plant expansion, although a slightly more contribution of C_4 plants to a predominately C_3 biomass could be indicated between 14.5 and 9.5 Ma. In the two study locations separated laterally by ~200 km along tectonic strike, this contrasting trend of vegetation change likely indicates local controls like riparian vegetation in the flood plain of the paleo-Karnali river and/or physical disturbance (e.g., fire) that would be worth exploring in future studies. Our study also suggests that the past vegetation makeup of an area is better constructed with isotopic signatures of molecular markers.

Key words: *Vegetation change, carbon isotope, lipid biomarkers, Siwalik, Himalayan foreland.*

Introduction:

Late Miocene global expansion of C_4 grasses over C_3 trees is extensively documented from various parts of the world including the Siwalik range, Himalayan foreland. Although the grass expansion likely started between 32 and 23 Ma (Fox and Koch, 2004; Edwards et al., 2010; Urban et al., 2010), the main expansion occurred in the Late Miocene (Quade et al., 1989, 1995; Cerling et al., 1993, 1997).

The expansion of C_4 plants tends to be asynchronous from one continent to another and even regionally within one continent. For example, this vegetation shift started between 6.4 and 4 Ma in the North American Great Plains (Fox and Koch, 2004) and around 2.6 Ma in the Gulf of Mexico region (Tipple and Pagani, 2010). The shift in East Africa occurred between 11 and 5 Ma (Feakins et al., 2013), but more likely over the past 6 Ma (Cerling et al., 2011). The timing of C_4 plant expansion in the Himalayan foreland was variously shown as between 7.4 and 7 Ma (Quade et al., 1989, 1995), 8 and 6.5 Ma (Hoorn et al., 2000), and between 7.9 and 5.5 Ma (Huang et al., 2007).

Most studies of the Neogene vegetation shift were based on the widely used proxy of carbon isotope of pedogenic carbonate nodules or bulk organic matter (e.g., Cerling et al., 1993; Quade et al., 1989, 1995; Fox and Koch, 2004). Only a few studies are based on the compound specific isotopic analysis (CSIA) (e.g., Huang et al., 2007; Tipple and Pagani, 2010). In the bulk carbon isotope study, the organic matter in the soil can receive input from organisms other than the vegetation, including insects, cyanobacteria, fungi and soil bacteria, as was reported in the Pakistani Siwalik (Freeman and Colarusso, 2001). Similarly, the diagenetic alteration of

carbonate nodules can also be a problem, as reported in the Siwalik succession in the Surai Khola section of Nepal (Sanyal et al., 2005).

In CSIA, we can specifically target refractory compounds or biomarkers, derived only from higher (i.e., vascular) plants, that have widespread distributions in terrestrial, lacustrine and marine sediments (Tipple and Pagani, 2007). Moreover, this method analyzes leaf wax lipid, which is largely resistant to diagenetic alteration (Sessions et al., 2004). The extraction of lipids following different chemical treatments allows to analyze isotopic values of individual carbons in a carbon chain. This technique was applied in the Tibetan Plateau by Polissar et al. (2009) and Liu et al. (2005), and in the Arabian Sea by Huang et al. (2007) to understand Neogene vegetation change.

For the Himalayan foreland, Freeman and Colarusso (2001) applied CSIA method in the Pakistani Siwalik, where they included additionally only two samples from the Nepalese Siwalik. Here, we present the first extensive studies of CSIA in the Nepalese Siwalik. We analyzed organic matter from paleomagnetically age-constrained mudstones and paleosols deposited in the Himalayan foreland basin during Middle Miocene to Early Pleistocene. The objective of this study is to test the applicability of CSIA in the Nepalese Siwalik and compare CSIA results with previously published bulk carbon isotope results from the same locality (Quade et al., 1995) for a better understating of the Late Neogene expansion of C_4 plants. This study also report new isotopic results from a previously undocumented locality, the Karnali River section of Nepal.

Geology of the study area:

The Himalayan rock successions are divided into four tectonostratigraphic units (Tethyan Himalaya, Higher Himalaya, Lesser Himalaya and Siwalik), which are separated from each other

by the north-dipping thrust fault systems (Figs. 2.1 A-B; Gansser, 1964; Hodges, 1988, 1996; DeCelles et al., 1998a,b). The youngest unit Siwalik is separated from the Lesser Himalayan rocks by MBT (Main Boundary Thrust) to the north, and from the Gangetic plain (present day foreland basin) by the (MFT (Main Frontal Thrust) to the south.

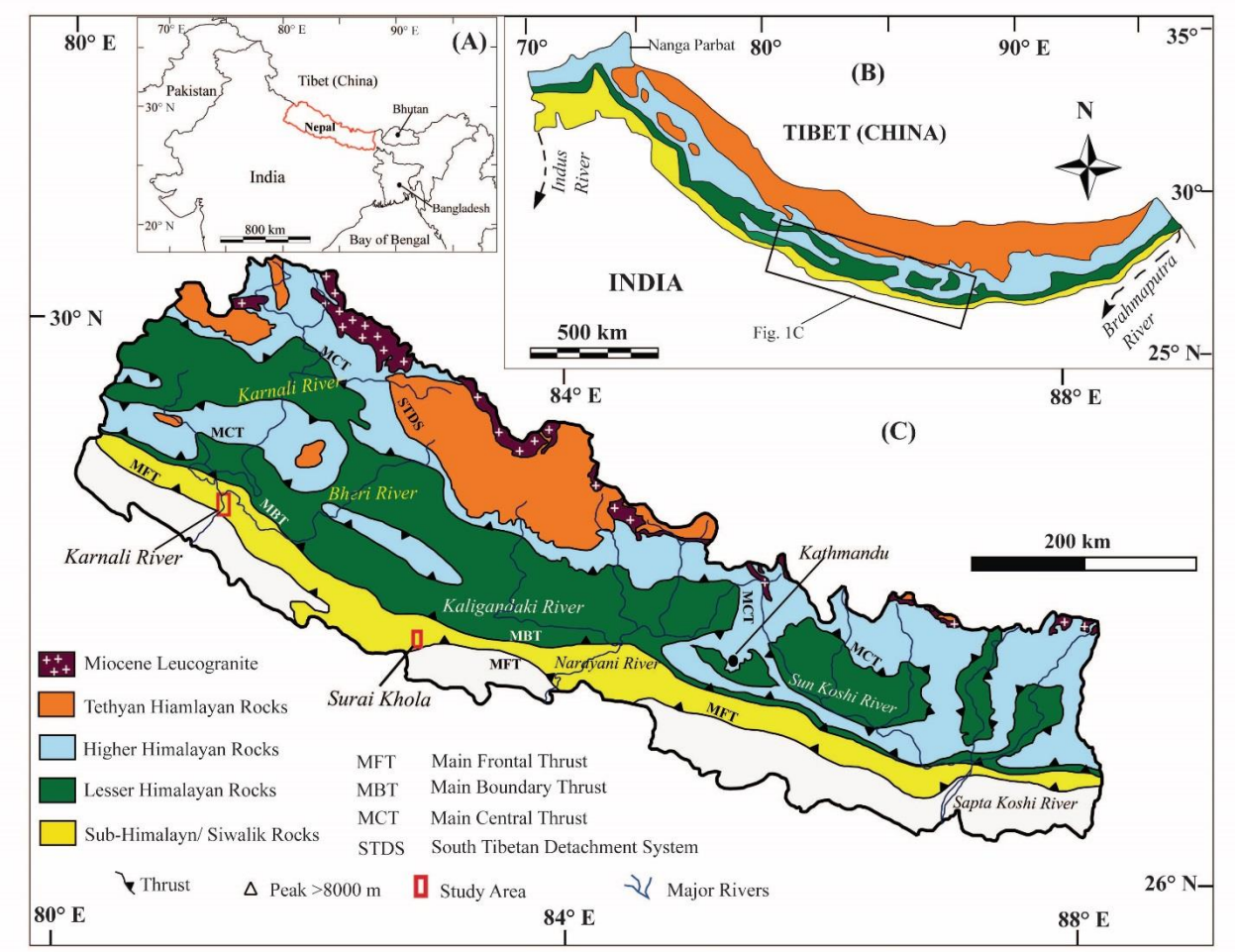

Figure. 2.1 (A) Outline Map of South Asia, showing Nepal in red boundary. (B) Regional geological map of the Himalaya from the Brahmaputra River in the east to the Indus River in the west. (C) Geological map of Nepal including all tectonostratigraphic rock units and major rivers. The two study locations are marked by red boxes in the Siwalik Rocks. (After Martin et al., 2005 and Corrie and Kohn, 2011).

Out of the ~2,000 km long Siwalik outcrop belt in the Himalayan foreland, the Nepal Siwalik itself has ~800 km long exposures along E-W (Fig. 2.1C), with an average total thickness of ~6 km (Schelling et al., 1991; Gautam et al., 2000). The molasse sedimentary rocks

of the Siwalik succession were deposited during the Miocene and the Early Pleistocene (Prakash et al., 1980; Burbank et al., 1996; Tokuoka et al., 1986; Appel et al., 1991; Gautam and Fujiwara, 2000; Ojha et al., 2000), and are now exposed in the foothill of Himalaya (Fig. 2.1C). Based on lithology, the Siwalik succession is divided into three units: Lower Siwalik, Middle Siwalik, and Upper Siwalik (Auden, 1935; Hagen, 1969; Yoshida and Arita, 1982; Ulak, 2009). The Lower Siwalik consists of interbedded of fine to medium grained, gray sandstone and variegated or gray mudstone (Fig. 2.2 A-B), which suggests fluvial and floodplain depositional environments (Gautam and Rösler, 1999; Ulak, 2009). The medium to coarse grained, "salt and pepper" sandstones, which are often multistory in nature and intercalated with mudstones (Fig. 2.2 C-D), indicate a braided river deposition in the Middle Siwalik (Gautam and Rösler, 1999; Nakayama and Ulak, 1999; Ojha et al., 2000; Ulak, 2009). On the other hand, the Upper Siwalik consists of bedded pebble and cobble conglomerates intercalated with loosely-packed sandstone and claystone layers that are interpreted to represent alluvial fan environments deposited closer the mountain belt (Gautam and Rösler, 1999; Ojha et al., 2000; Ulak, 2009).

Several paleomagnetic studies were conducted in the Nepalese Siwalik to reveal high-resolution ages of the Siwalik succession. These studies indicate that the Siwalik ranges in age from 16 to 2 Ma (Appel et al., 1991; Gautam and Rösler, 1999; Gautam and Fujiwara, 2000; Ojha et al., 2009). For this study, we selected two well exposed and paleomagnetically age-constrained river sections, where organic-rich sedimentary rock samples were collected for carbon isotope study (Fig. 2.1C). These two along tectonic-strike sections are Surai Khola, which exposes 13 to 2 Ma old strata (Appel et al., 1991), and Karnali River, which exposes 16 to 5.2 Ma old strata (Gautam and Fujiwara, 2000).

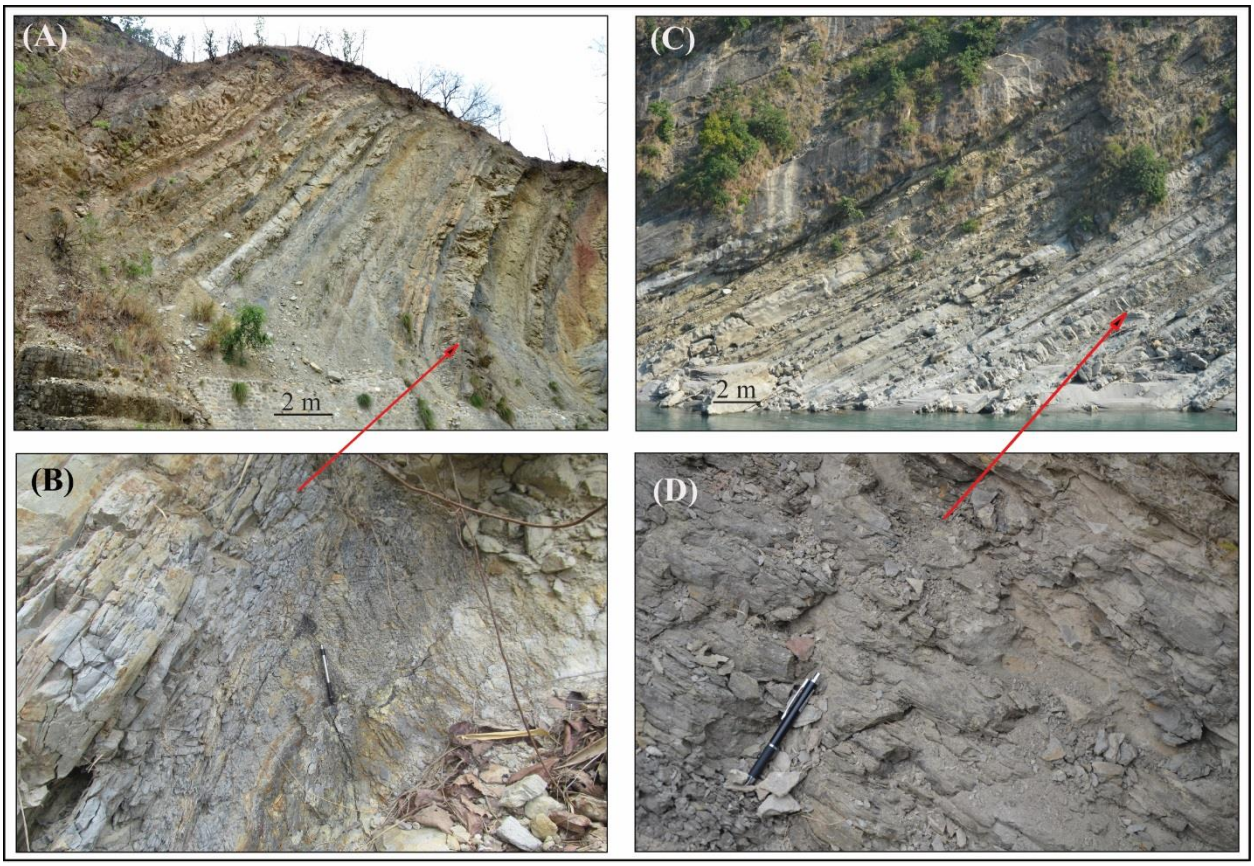

Figure 2.2. Siwalik fluvial sedimentary rocks in Nepal. (A) Lower Siwalik exposure in the Surai Khola section, showing sandstone interbedded with mudstone. (B) Close-up view of a mudstone bed. (C) Middle Siwalik exposure in the Karnali River section, showing interbedded sandstone and mudstone. (D) Close-up view of a floodplain mudstone bed.

Methodology:

With the help of the detailed log data that were generously provided to us by the senior authors of previous paleomagnetic studies at the Surai Khola and Karnali River sections (Appel et al., 1991; Gautam and Fujiwara, 2000), we identified most of the paleomagnetic sample holes, where a few missing holes were located with the help of bearing and thickness data. These paleomagnetic ages are based on the time scale of Cande and Kent (1995).

A total of 47 samples, mostly floodplain mudstones and some paleosols, were collected (28 from Karnali River and 19 from Surai Khola) with a regular sampling interval, averaging of

0.5– 0.25 Ma. Samples were chemically analyzed in the organic geochemistry lab at the Brown University for CSIA study. For sample preparation and chemical treatment, we followed the procedure described in Liu et al. (2005) and Gao et al. (2011).

Samples were first cleaned three times with dichloromethane to remove any possible surface contamination and freeze-dried for 12 hours. The dried samples were grinded in a ceramic pestle with mortar, weighted to collect 40–60 gm and then mixed with baked sands (2:1) to enhance the mobility of organic compounds. Prepared samples were placed in an ASE 200 (Accelerated Solvent Extractor) and organic materials were collected in 40 ml glass vials using dichloromethane: methanol (9:1) solution at 120° C with 1200 psi. Extracted organic materials were separated into acid and neutral fractions by using silica-based LC-NH_2 column, and dichloromethane: isopropanol (2:1) and ethyl-ether: acetic-acid (96:4) solutions. The neutral fractions of organic compounds were again eluted in silica gel column (LC-SiO_2) with hexane solution to obtain *n*-alkanes, which were then run into a gas chromatograph and fame ionization detector (GC-FID) to identify the concentration of organic compounds in the analyzed samples. Identification of specific compounds was based on the comparison of mass spectra from GC-MS (gas chromatography-mass spectrometry) with respect to GC retention times (Gao et al., 2011). Finally, organic compounds (*n*-alkane fractions) were run in a HPCL-MS to obtain compound specific $\delta^{13}C$ values.

In vegetation shift (C_3 vs. C_4 plants) study using sedimentary samples, $\delta^{13}C$ in various materials, including organic matter, lipid biomarker and soil carbonate, is used as a proxy. In soil carbonates (carbonate nodules), $\delta^{13}C$ value ranges from -14‰ to -8‰ for C_3 plants, and > -8‰ for C_4 plants (Quade et al., 1989). For bulk organic matter, modern C_3 plants have a wide range of $\delta^{13}C$ values ranging from -35‰ to -20‰, whereas C_4 plants have shorter range between

-14‰ and -10‰ (Tipple & Pagani, 2007). In lipid biomarkers, *n*-alkane $\delta^{13}C$ shows an average value of -36‰ for modern C_3 plants, whereas the average value range from -24‰ to -20‰ for C_4 plants (Collister et al., 1994; Tipple & Pagani, 2007). In this study, these values are used as general guidelines while interpreting the data with an assumption that $\delta^{13}C$ of Miocene atmospheric CO_2 was similar to preindustrial values.

Results:

Here, we present CSIA results from lipid biomarkers extracted from terrestrial mudstones and paleosols deposited during Neogene in the flood-plain environment. Generally, organic matter deposited in a flood-plain environment is sourced from nearby and upstream biota. In this study, we focus on the odd number long-chain carbons (C_{27} to C_{31}) of *n*-alkanes, which come from terrestrial higher plants (Eglington and Hamilton, 1967; Tipple and Pagani, 2007; Sachse et al., 2012), as opposed to lower chain-length *n*-alkanes ($<C_{25}$) that are commonly from aquatic plants and algae (Ficken et al., 2000; Gao et al., 2011). Our $\delta^{13}C$ values of C_{27}, C_{29} and C_{31} *n*-alkanes are strongly correlated with each other, and we refer to the value of C_{27} in describing our result. The chromatographs of *n*-alkane lipids show regular peaks with a strong odd-over-even preference (Fig. 2.3), indicating insignificant thermal alteration of the analyzed organic matter.

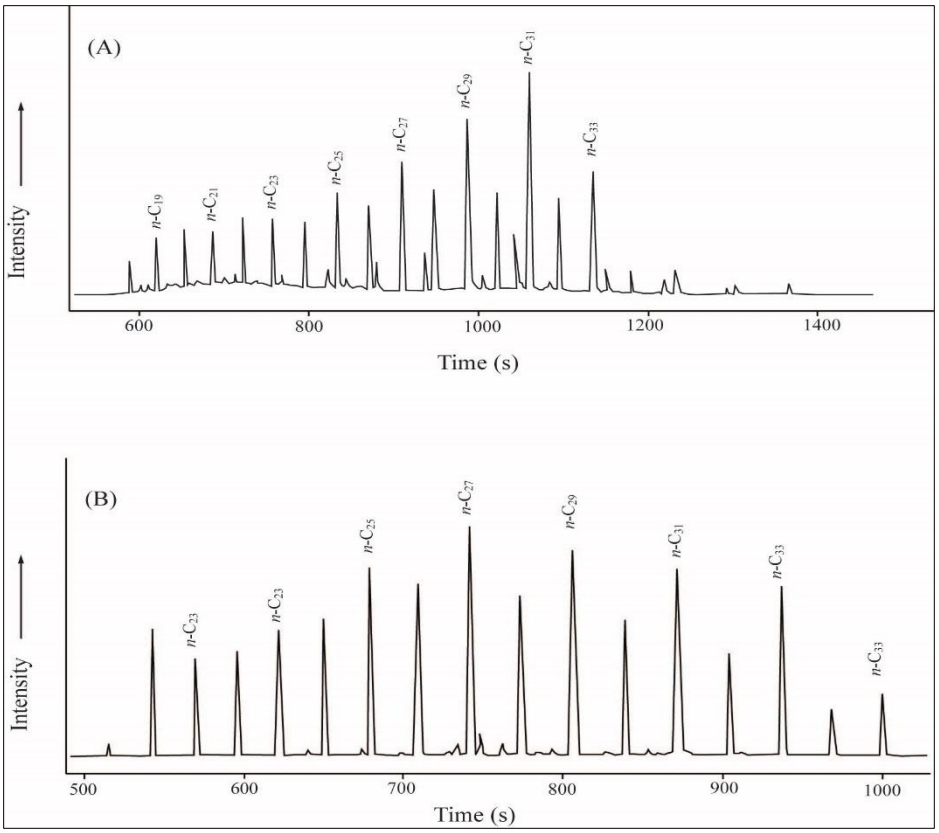

Figure 2.3. Representative chromatographs of *n*-alkanes for Karnali River (A) and Surai Khola (B) samples, both of which are floodplain mudstones.

Surai Khola section:

$\delta^{13}C$ values of C_{27} range from -32.3‰ to -18.7‰ with an average of -25.5‰ in the Surai Khola section (Table 2.1). The oldest sample (12 Ma) has a $\delta^{13}C$ value of -29.2‰, and the maximum depletion was recorded around 10 Ma (-32.3‰). From 12 to 8.5 Ma, the values show a fluctuating trend with an overall decrease of ~2‰. From 8.5 to 6.5 Ma, the values show a slow yet steady increase by ~2‰. The $\delta^{13}C$ values started to increase abruptly at 6.5 Ma (Fig. 2.4), where the values increase dramatically by ~6‰ to reach -23.6‰ at 5.2 Ma. From 5.2 to 2.5 Ma, our data show a higher-amplitude $\delta^{13}C$ variability (Fig. 2.4C) with an overall increase by ~4‰ to reach -19.1‰ at 2.5 Ma.

Table 2.1. $\delta^{13}C$ values of *n*-alkane C_{27}, C_{29} and C_{31} for Surai Khola samples.

		$\delta^{13}C$ *n*-alkane (‰)		
Sample #	Age (Ma)	C_{27}	C_{29}	C_{31}
13-NP-SK-29	2.50	-19.09	-19.72	-18.95
13-NP-SK-30	3.00	-24.55	-26.79	-24.87
12-NP-SK-26	3.85	-18.67	-18.96	-18.66
12-NP-SK-25	4.70	-26.22	-28.12	-25.27
12-NP-SK-24	5.20	-23.64	-25.62	-25.96
12-NP-SK-16	5.40	-26.96	-26.84	-33.92
12-NP-SK-15	5.55	-26.76	-25.65	-23.34
12-NP-SK-14	6.05	-28.34	-27.22	-25.31
12-NP-SK-13	6.50	-29.51	-30.39	-31.77
12-NP-SK-11	7.00	-29.78	-30.01	-29.33
12-NP-SK-10	7.50	-29.75	-30.56	-31.18
12-NP-SK-9	8.00	-30.08	-30.05	-29.89
12-NP-SK-7	8.50	-31.14	-31.45	-32.59
12-NP-SK-5	9.00	-30.10	-30.47	-32.42
12-NP-SK-4	9.50	-30.53	-30.68	-31.76
12-NP-SK-2	10.00	-32.33	-32.95	-34.31
12-NP-SK-23	10.80	-28.03	-29.21	-31.80
12-NP-SK-22	11.20	-30.44	-30.76	-31.89
12-NP-SK-20	11.95	-29.19	-29.21	-30.45

Karnali River section:

$\delta^{13}C$ values of *n*-alkane C_{27} range from -32.8‰ to -27.8‰ with an average of -30.3‰ in the Karnali River section (Table 2.2). The oldest sample of 16 Ma shows a $\delta^{13}C$ value of -29.6‰ that decreases by ~2‰ at 14.5 Ma. For the first time, the values start to increase after 14.5 but remains consistent around -28‰ until 9.5 Ma. From 9.5 to 5.2 Ma (the youngest sample age), the values show a high-amplitude $\delta^{13}C$ fluctuations (Fig. 2.4C) in the range of ~3‰. Notably during this time, the $\delta^{13}C$ values also show an overall depleting trend by ~3‰.

Table 2.2. $\delta^{13}C$ values of *n*-alkane C_{27}, C_{29} and C_{31} for Karnali River samples.

		$\delta^{13}C$ *n*-alkane (‰)		
Sample #	Age (Ma)	C_{27}	C_{29}	C_{31}
13-NP-KR-50	5.20	-30.02	-31.91	-34.30
13-NP-KR-49	5.25	-32.78	-32.43	-46.33
13-NP-KR-48	5.50	-30.46	-33.50	-36.14
13-NP-KR-47	5.90	-31.92	-32.80	-34.15
13-NP-KR-46	6.00	-31.79	-33.34	-35.19
13-NP-KR-44	6.25	-31.90	-31.64	-34.08
13-NP-KR-43	6.40	-28.57	-30.85	-33.43
13-NP-KR-42	7.00	-28.15	-29.19	-30.54
13-NP-KR-41	7.25	-31.76	-32.81	-35.41
13-NP-KR-40	7.50	-31.43	-32.12	-33.18
13-NP-KR-39	7.75	-28.96	-30.17	-32.03
13-NP-KR-38	8.00	-29.67	-30.72	-31.89
13-NP-KR-37	8.25	-30.79	-30.90	-32.85
13-NP-KR-36	8.50	-31.05	-31.68	-32.76
13-NP-KR-35	8.75	-31.75	-31.69	-34.11
13-NP-KR-34	9.00	-30.14	-31.27	-33.05
13-NP-KR-32	9.50	-28.04	-28.95	-29.83
13-NP-KR-29	10.25	-27.80	-28.68	-30.63
13-NP-KR-28	10.50	-28.06	-28.28	-28.68
13-NP-KR-25	11.25	-28.30	-29.18	-32.15
13-NP-KR-22	12.00	-28.87	-29.52	-30.78
13-NP-KRa-22	13.00	-28.46	-29.54	----
13-NP-KRa-20	13.50	-28.20	-28.31	----
13-NP-KR-18	14.00	-28.76	-29.12	-29.90
13-NP-KR-16	14.50	-31.22	-31.25	-31.36
13-NP-KR-14	15.00	-31.02	-32.21	-32.72
13-NP-KR-13	15.40	-30.19	-32.11	-32.15
13-NP-KR-11	16.00	-29.63	-33.19	-32.79

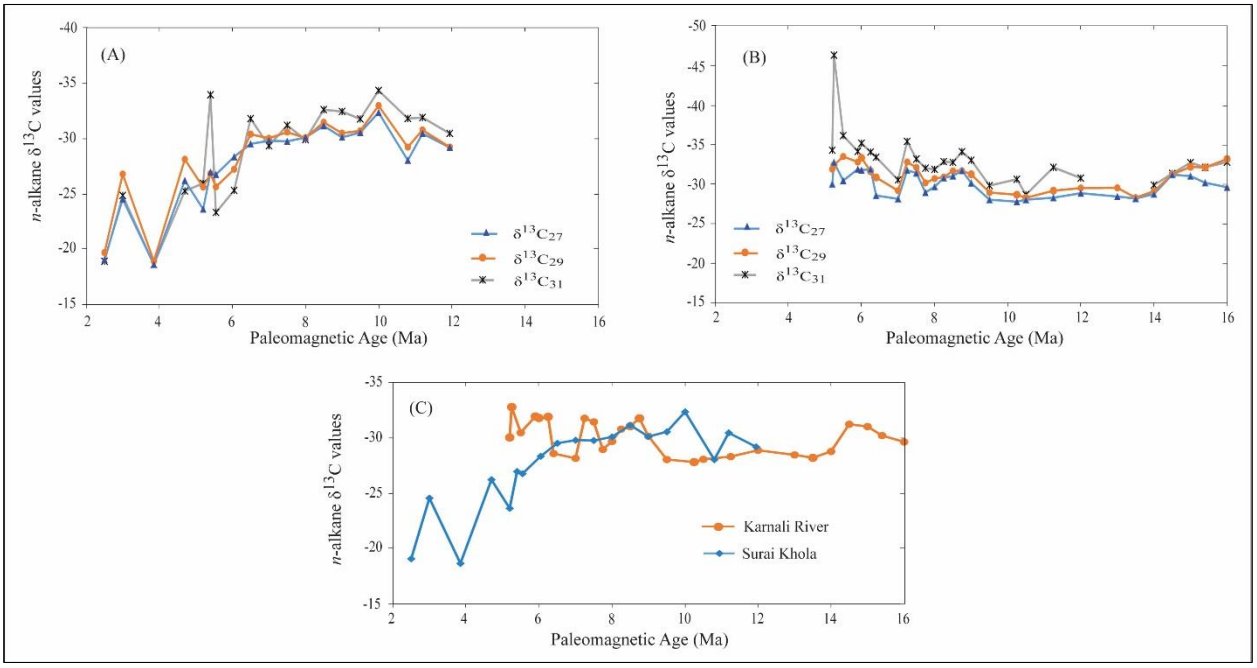

Figure 2.4. (A) & (B) $\delta^{13}C$ *n*-alkane of C_{27}, C_{29} and C_{31} from the Surai Khola and Karnali River sections, respectively. (C) Comparison of $\delta^{13}C$ values of C_{27} from both the Surai Khola and Karnali River sections.

Discussion:

In the Himalayan foreland, previous isotopic studies of the Neogene vegetation shift from C_3 plants to C_4 plants used Siwalik paleosols or fossil teeth, which generally have a limited stratigraphic occurrence. To overcome this limitation, other isotopic studies used marine sediments from the Bay of Bengal and Arabian Sea (Freeman and Colarusso, 2001; Huang et al., 2007). However, organic materials transported to marine basins from upstream continental lands represent a regionally-integrated signal of the terrestrial ecosystem (Tipple and Pagani, 2007). On the contrary, here we used both mudstone and paleosol samples collected from the terrestrial Siwalik strata at a regular and high-resolution interval of 0.5– 0.25 Myr. Moreover, we also applied molecular-specific (as opposed to bulk) carbon isotopic analysis. Therefore, our data

have more potential of revealing a proximate as well as direct evidence for the character of ancient vegetation and their temporal changes in the Himalayan foreland.

Many previous studies used $\delta^{13}C$ as a robust proxy for terrestrial vegetation types in the Himalayan regions (Quade and Cerling, 1995; Quade et al., 1995; Freeman and Colarusso, 2001; Huang et al., 2007; Behrensmeyer et al., 2007; Sanyal et al., 2010). Similarly, we argue that our $\delta^{13}C$ data of *n*-alkane lipids extracted from floodplain strata reflect past vegetation character in the region. Our $\delta^{13}C$ values of C_{27} of the Surai Khola section suggest a C_3 plant domination between 12 and 8.5 Ma (Table 2.1; Fig. 2.4C). C_4 plant likely started to expand gradually at 8.5 Ma and rapidly at 6.5 Ma. By 5.2 Ma, C_4 vegetation clearly dominated the landscape, as suggested by a heavily enriched $\delta^{13}C$ value of -23.6‰. Maintaining this dominance, C_4 plants continued to expand between 5.2 and 2.5 Ma. However, higher-amplitude $\delta^{13}C$ fluctuations during this time (Fig. 2.4C) likely indicate that patches of C_3 forest expanded and contracted several times.

Overall, our lipid biomarker study of the Surai Khola section validates the results of Quade et al. (1995), who used $\delta^{13}C$ of pedogenic carbonate nodules and bulk organic matter from the same section to document the late Miocene vegetation shift from C_3 plants to C_4 plants (Fig. 2.5). However, several differences are notable. Our data have relatively less scatter with clearer trend of vegetation change, which likely reflects the fact that molecule-specific biomarker proxy can specifically target organic matter sourced from terrestrial higher plants (Tipple and Pagani, 2007; Freeman and Colarusso, 2001). In this respect, our study supports the finding of Freeman and Colarusso (2001) that the history of terrestrial vegetation makeup is better constructed with isotopic signatures of molecular markers. Although Quade et al. (1995) data suggest a dramatic expansion of C_4 plants replacing C_3 plants around 7 Ma, our data indicates a

stepwise expansion of C_4 plants starting gradually at 8.5 Ma and culminating rapidly at 5.2 Ma (Fig. 2.5).

This study presents the first isotopic data in the Karnali River section. Our $\delta^{13}C$ values of C_{27} suggest a different scenario of vegetation history in the Karnali River section (Table 2.2; Fig. 2.4C) than what is interpreted from the Surai Khola data. No clear sign of C_4 plant expansion is indicated in the Karnali River section till 5.2 Ma, which is the age of our youngest sample in this section. However, a slightly more contribution of C_4 plants to a predominately C_3 biomass could be indicated between 14.5 and 9.5 Ma (Fig. 2.4C). While Surai Khola data suggest expansion of C_4 plants for the past 8.5 Ma, Karnali River data indicate expansion of rather C_3 plants between 9.5 and 5.2 Ma. This opposite trend of vegetation shift around 9 Ma in two different areas separated laterally by ~200 km along tectonic-strike is intriguing.

The growing literature of the late Neogene vegetation shift is increasingly advocating asynchronous and spatially-heterogeneous expansion of C_4 plants replacing C_3 community in the Himalayan foreland. In the Pakistani Siwalik, based on $\delta^{13}C$ of soil carbonate and bulk organic matter, previous studies showed a transition from C_3 to C_4 vegetation between 8 and ~5 Ma (Quade and Cerling, 1995; Behrensmeyer et al., 2007). Similarly, $\delta^{13}C$ of carbonate nodules in the Indian Siwalik suggests appearance of C_4 plants asynchronously in various areas between 9 and 6 Ma (Sanyal et al., 2004, 2005, and 2010). Our lipid biomarker study in the Nepalese Siwalik suggests expansion of C_4 vegetation between 8.5 and 5.2 Ma in the Surai Khola section, yet no definite sign of C_4 plant expansion (till 5.2 Ma) in the Karnali River section (Fig. 2.4C). With a low pCO_2 as a likely necessary precondition, the asynchronous and spatially-heterogeneous late Neogene expansion of C_4 vegetation can be better explained with region-specific climatic factors (seasonal precipitation, aridity, temperature) and disturbances (fire,

herbivory) (Tipple and Pagani, 2007; Stromberg, 2011). In addition, local environments like riparian vegetation along river banks can be responsible for anomalous presence of C_3 vegetation in the Siwalik floodplain (e.g. Behrensmeyer et al., 2007). For the Karnali river section, we speculate that such might be the case for the existence of C_3 riparian-vegetation along the paleo-Karnali river as late as 5.2 Ma.

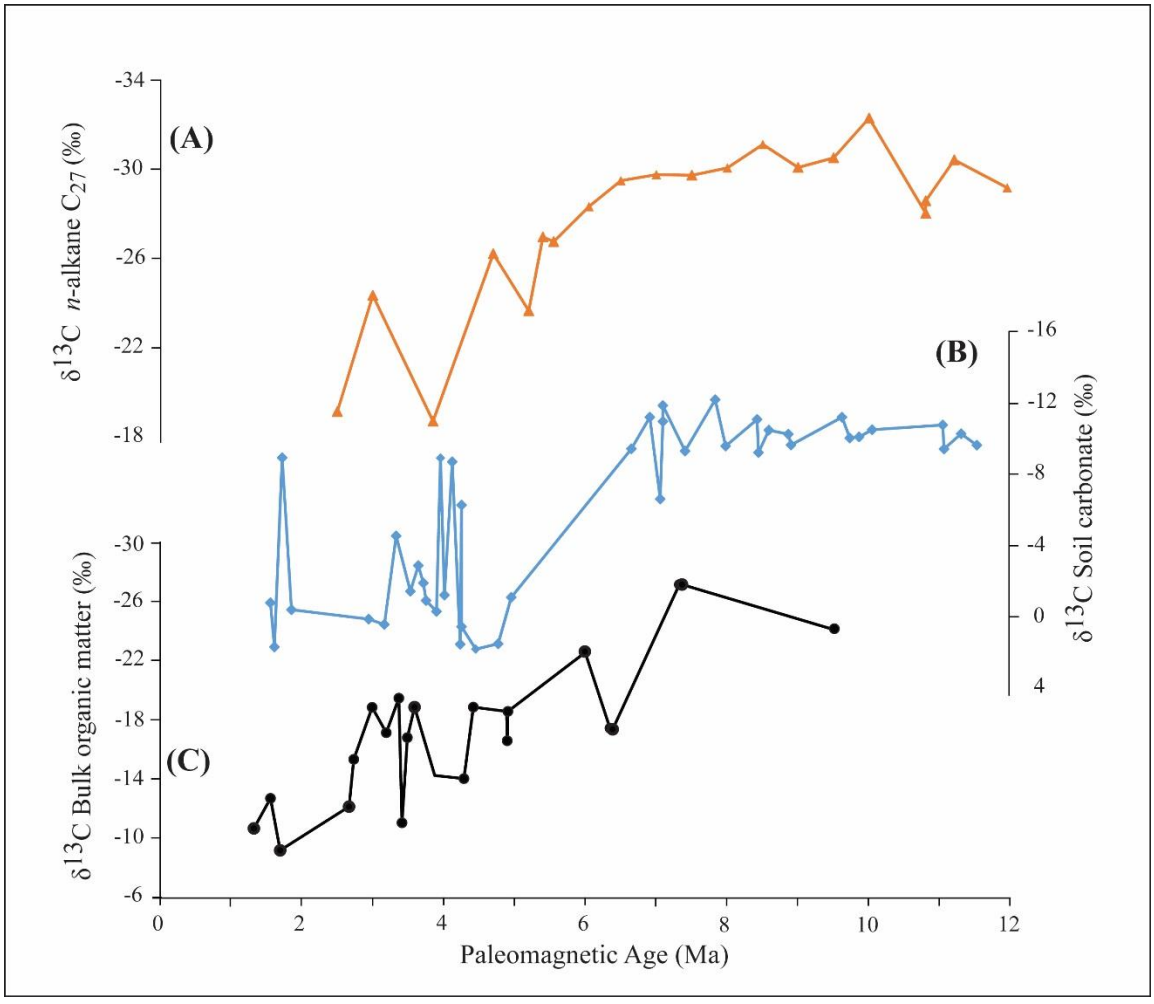

Figure 2.5. Correlation of lipid biomarker data of this study (A) with Quade et al. (1995) data (B and C) from the Surai Khola section.

Conclusions:

There are two main advantages of molecular-specific lipid biomarker approach of carbon isotope in reconstructing past vegetation history: ability to specifically target terrestrial higher (i.e., vascular) plants, and sampling is not restricted to paleosols or fossil teeth. Here, we used $\delta^{13}C$ of *n*-alkanes (C_{27-31}) extracted from floodplain shale and paleosols in the Nepalese Siwalik for a better knowledge of the Neogene vegetation shift from C_3 to C_4 plants.

Broadly, our data from the Surai Khola section support the results of Quade et al. (1995), who used $\delta^{13}C$ of pedogenic carbonate nodules and bulk organic matter from the same section to document the vegetation shift. However, unlike a dramatic expansion of C_4 plants around 7 Ma that was suggested previously, our data indicates a stepwise expansion of C_4 vegetation starting gradually at 8.5 Ma and culminating rapidly at 5.2 Ma. We also present first isotopic data from the Karnali River section. While Surai Khola data suggest expansion of C_4 plants for the past 8.5 Ma, Karnali River data indicate expansion of rather C_3 plants between 9.5 and 5.2 Ma. This opposite trend of vegetation shift around 9 Ma in two different locations separated laterally by ~200 km along tectonic-strike is worth exploring further.

Chapter 3

Constraining Neogene climate variability using multiproxy isotopic study of the Siwalik rocks, Nepalese Himalaya

Abstract:

Mudstone and paleosol samples collected from the Surai Khola and the Karnali River sections of the Neogene foreland basin strata (Siwalik) in Nepal were chemically analyzed and studied for the compound specific isotope analysis (CSIA) of carbon and hydrogen along with glycerol dialkyl glycerol tetraether (GDGTs). The carbon isotope data of the Surai Khola section indicates that the C_4 greasses gradually expanded since 8.5 Ma and became dominant by 5.5 Ma. However, in the Karnali River section, although some contribution of C_4 plants are identified between 14.5 and 9.5 Ma, no clear sign of C_4 grass expansion is observed.

δD data indicate two phases of rainfall intensification in the Surai Khola section- one around 10 Ma and the other around 5.5 Ma. Contrary to previous publications, our δD values indicate an overall increase in rainfall amount towards the younger age. The negative correlations between rainfall and GDGT-derived temperature before 5.5 Ma suggest that the region experienced higher rainfalls during period of lower annual temperatures and vice versa. The modern day rainfall pattern in the Indian subcontinent shows higher amount of rainfall during the hot summer than during cold winter. We propose that the negative correlation between rainfall and mean annual air temperature (MAAT) prior to 5.5 Ma could be related to the strong presence of mid-latitude westerlies in the region, when summer monsoon winds were weaker, that brought enhanced winter-precipitation particularly during colder periods. After 5.5 Ma, our data show a conspicuous positive correlation between rainfall and annual temperature, indicating the onset of modern-style seasonality in rainfall in the Indian subcontinent.

Keywords: *Multiproxy; lipid biomarkers, Neogene; vegetation shift; Siwalik; Indian monsoon*

Introduction:

Various geochemical signatures in the terrestrial sedimentary rocks are valuable proxies in the study of paleoclimate and paleoecology. Particularly in the Indian subcontinent, scientists have used a number of geochemical climate proxies to reveal the nature and causes of the Neogene climate changes (Quade et al., 1989, 1995; Dettman et al., 2001; Gupta et al., 2004; Sanyal et al., 2010; Singh et al., 2012). The climate proxies such as carbon and oxygen isotopes (Quade et al., 1989; 1995; Quade and Cerling, 1995; Freeman and Colarusso, 2001; Behrensmeyer et al., 2007; Huang et al., 2007; Sanyal et al., 2010; Singh et al,. 2012), hydrogen isotopes (Ghosh et al., 2004; Huang et al., 2007; Sanyal et al., 2010), fossils (Konomatsu, 1997; Dettman et al., 2001), and chemical weathering and sedimentation rates (Clift et al., 2008) are previously used for paleoclimate studies of the region. These previous studies of the Himalayan region have provided valuable insights on evolution of climate over time; however, there are some ongoing debates on several issues. Specifically, the issues related to the timing and mechanisms for the changes in vegetation (i.e., C_4 grasses replacing C_3 trees), and the initiation and/or intensification of south Asian monsoon (with rainfall whether increasing or decreasing) are not yet completely resolved.

Majority of the previous carbon isotope ($\delta^{13}C$) studies conducted on the Siwalik sediments showed incongruent timing for the vegetation shift from C_3 to C_4 type. For example, Quade et al. (1989, 1995) reported that the vegetation shift occurred between 7.4 and 7 Ma in Pakistan and Nepal, whereas Hoorn et al. (2000) argued that the transition occurred between 8 and 6.5 Ma. Similarly, Freeman and Colarusso (2001) suggested that the vegetation transition was initiated at ca. 9 Ma and completed between 8 and 6 Ma. Other researchers, such as Behrensmeyer et al. (2007), Huang et al. (2007), and Sanyal et al. (2010) advocated that the vegetation shift occurred at 8 - 4 Ma, , 7.9 - 5.5 Ma, and 6 Ma, respectively.

Similarly, rainfall proxies such as $\delta^{18}O$ and δD of the Siwalik strata pointed an incongruent mode and tempo of the rainfall intensifications. Quade et al. (1989, 1995) and Quade and Cerling (1995) reported a strong rainfall intensification in the region around 7 Ma. Subsequently, Dettman et al. (2001) suggested an earlier (ca.11 Ma) occurrence of such a rainfall intensification event; however, Sanyal et al. (2010) identified three phases of monsoon intensifications that occurred at 11, 6, and 3 Ma. Singh et al. (2012) concurred with Sanyal et al. (2010) on three phases of intensifications but differed on timings such that these intensifications occurred ca. 10, 5 and 1.8 Ma. Meanwhile, using the sedimentation rate in the distal part of the Bengal fan, Clift et al. (2008) identified two phases of monsoon intensifications between 15 and 10.5 Ma and around 3.5 Ma.

$\delta^{13}C$ and $\delta^{18}O$ from pedogenic carbonate nodules or bulk organic matter were the most commonly used climate proxies in previous studies (Quade et al., 1989, 1995; Quade and Cerling, 1995; Sanyal et al., 2010; Singh et al., 2012), whereas only a few studies used compound specific lipid biomarkers as a proxies (Freeman and Colarusso, 2001; Huang et al., 2007). In the bulk isotope study, the high likelihood of diagenetic alterations of carbonate nodules in the ~6 km thick successions of Siwalik rocks can be problematic for data interpretation. For example, diagenetic alteration is reported in the Surai Khola section of the Nepalese Siwalik (Sanyal et al., 2005). Furthermore, pedogenic carbonate formation is highly sensitive to evaporation (Polissar et al., 2009). Similarly, in the bulk carbon isotope studies of organic matters, it is difficult to identify the various source of organic materials received by the soil other than vegetation. Such sources may include insects, cyanobacteria, fungi and soil bacteria as reported by Freeman and Colarusso (2001) in Pakistani sections of the Siwalik. On the other hand, the Neogene Himalayan paleoclimate studies based on sedimentological,

chemical, and isotopic proxies retrieved from the drilling cores of the Bengal Fan (Clift et al., 2008) and Arabian Sea (Huang et al., 2007) might represent regionally integrated signals of the terrestrial ecosystem (Tipple and Pagani, 2007) rather than representing direct local records.

Although paleotemperature constitutes an important part of the past climate reconstruction, previous studies rarely investigated paleotemperature of the region with little success. Based on the lowest $\delta^{18}O$ values from modern groundwater and lowest $\delta^{18}O$ values of soil carbonate from the upper part of the Surai Khola section, Quaide et al. (1995) estimated a Neogene paleotemperature of 26.5 °C. Sanyal et al. (2010) attempted a temperature measurement based on the $\delta^{18}O$ from modern precipitation and $\delta^{18}O$ from soil carbonate, but the Neogene temperature was abnormally high (39 °C). A recent study of Quade et al. (2013) showed that paleotemperature estimation based on clumped isotope of paleosol carbonate is unreliable for the Siwalik strata of ages >6 Ma because of the diagenetic resetting of clumped isotope values.

The main objective of the present study is to present a deeper insight on Neogene climate changes in the Himalayan foreland region using paleoclimate proxies derived from the compound specific isotope analysis (CSIA) of the lipid biomarkers extracted from the mudstone/paleosol samples. We intended to minimize data uncertainties and to reveal multiproxy interpretation of the paleoclimate and ecological changes in the Siwalik by collecting samples at a high-resolution interval from the paleomagnetically age constrained sections of the Siwalik – the Surai Khola (Appel et al., 1991) and the Karnali River (Gautam and Rösler, 1999; Gautam and Fujiwara, 2000). Specifically, we used microbially derived branched glycerol dialkyl glycerol tetraether (brGDGT) as a temperature proxy, and compound specific measurement of $\delta^{13}C$ (vegetation proxy) and δD (precipitation proxy) for the first time in the Siwalik. The isotope data were used to understand the changes in mean annual air temperature (MAAT),

vegetation (from C_3 trees to C_4 grasses), and rainfall/monsoon intensification in the Neogene foreland basin.

Geology of the study area:

The Himalayan orogeny started around 55 Ma with a collision between the Indian and Asian plates (Gansser, 1964; Rowely, 1996; Clift, 2008). Over time, the Himalaya began to rise in phases: such as ca. 55 Ma (Hodges, 2000), at ca. 34 Ma and ca. 20 Ma (Aitchison et al., 2007), between 45 to 55 Ma and < 23 Ma (Clift et al., 2008), and around 2.4 Ma (Sorkhabi et al., 1996) with the formation of major south-propagating thrusts (Catlos et al., 2001, 2002; Huyghe et al., 2001). The exhumed Himalayan rocks are being eroded, transported, and deposited by multiple rivers in the foreland basin to the south (Dickinson, 1985; DeCelles and Giles, 1996; Khanal and Robinson, 2013).

The south-propagating and north-dipping structural discontinuities (i.e., thrust faults) characterize the Himalayas into four tectonostratigraphic units: Tethys Himalaya, Higher Himalaya, Lesser Himalaya and sub-Himalaya or Siwalik (Gansser, 1964; Guchs and Frank, 1970; Upreti, 1999). From north to south, these Himalayan tectonostratigraphic units are separated from each other and the Gangetic Plain to the south by the South Tibetan Detachment System (STDS), Main Central Thrust (MCT), Main Boundary Thrust (MBT), and Main Frontal Thrust (MFT) (Fig. 3.1).

The southernmost ~2000 km long tectonostratigraphic unit (Siwalik) represents one of the most extensive Neogene foreland basin succession with thick fluvial deposits. The succession is well exposed in the Himalayan front along the major river sections throughout the Himalaya (Fig. 3.1). One third length of this Siwalik unit is located in Nepal with an average thickness of ~6 km (Schelling et al., 1991; Gautam and Rösler, 1999).

The Siwalik sediments were deposited between middle Miocene to early Pleistocene (Prakash et al., 1980; Burbank et al., 1996; Tokuoka et al., 1986; Appel et al., 1991; Gautam and Fujiwara, 2000; Ojha et al., 2000). In general, the coarsening-upward succession of the Siwalik are divided into three lithostratigraphic units: Lower Siwalik (LS), Middle Siwalik (MS) and Upper Siwalik (US) (Auden, 1935; Hagen, 1969; Yoshida and Arita, 1982; Rao et al., 1988; Gautam and Rösler, 1999; Ulak, 2009). The Lower Siwalik (Fig. 3.2 A-D) is characterized by flood plain deposits of variegated and bioturbated mudstone layers that are interbedded with very fine- to medium-grained, gray sandstone beds (Gautam and Rösler, 1999; Nakayama and Ulak, 1999; Ulak, 2009).

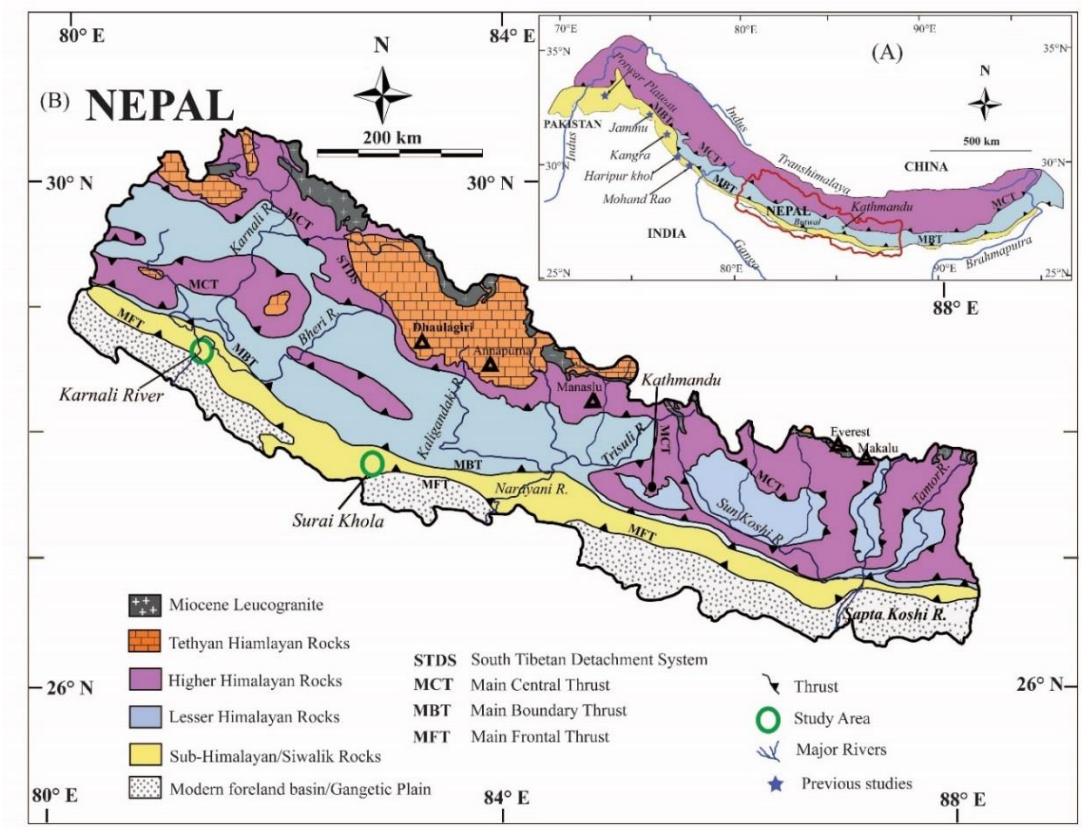

Figure 3.1. (A) Geological map of the Himalaya showing Nepal in red boundary. Location of previous studies are marked by stars (modified after Gansser, 1964; Gautam et al., 2000). (B) Geologic map of Nepal showing different tectonostratigraphic units. The present study (sample locations are marked with green circles) is focused on the Neogene Siwalik rocks (yellow) (modified after Martin et al., 2005; Corrie and Kohn, 2011).

The Middle Siwalik contains medium- to coarse-grained, mica-rich, multistory sandstone beds (Fig. 3.2B) with interbeds of mudstone deposited by braided river systems (Gautam and Rösler, 1999; Nakayama and Ulak, 1999; Ojha et al., 2000; Ulak, 2009). Similarly, the Upper Siwalik (Fig. 3.2 C) alluvial fan deposits consisting of tens of meters thick pebble and cobble conglomerates beds with some loose, boulder conglomerate, claystone, and grey sandstone layers (Gautam and Rösler, 1999; Nakayama and Ulak, 1999; Ojha et al., 2000; Ulak, 2009).

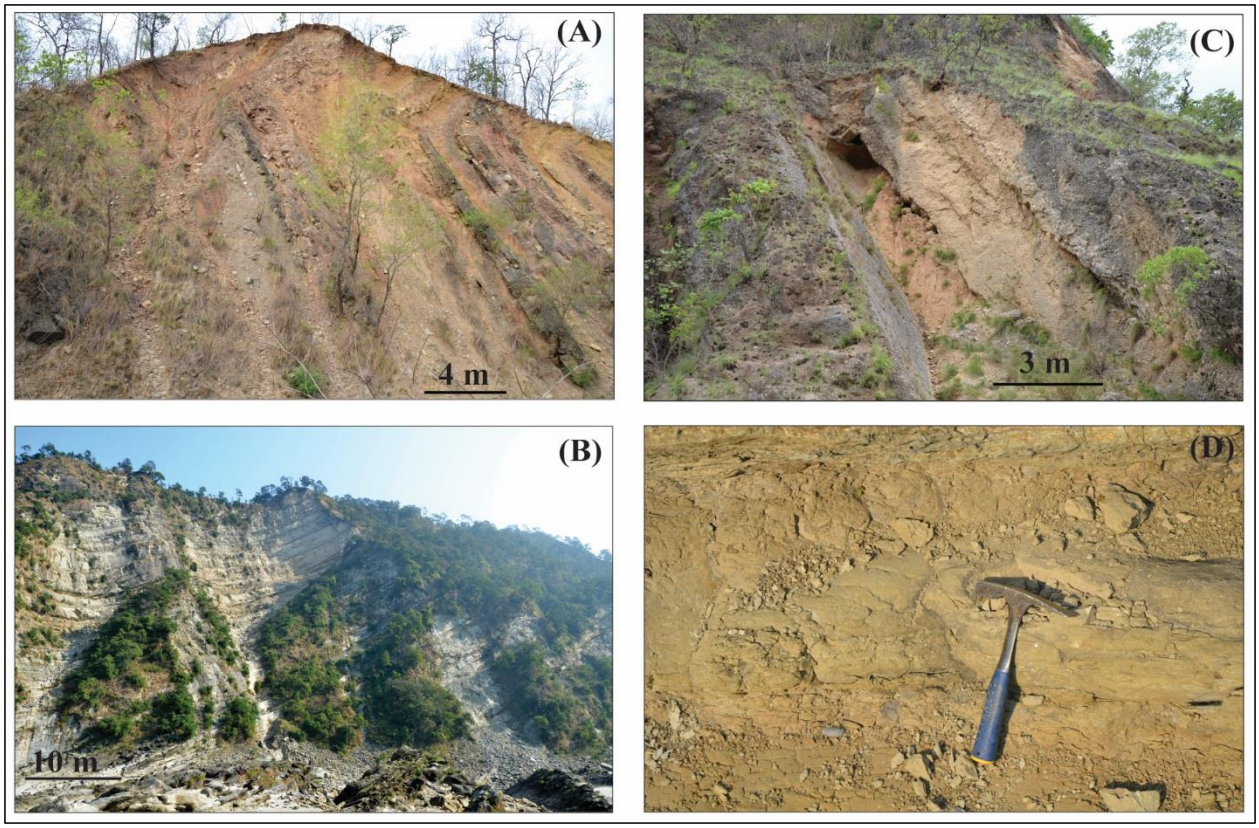

Figure 3.2. (A) Variegated mudstones (light yellow) interbedded with fine-grained sandstone beds (dark brown) in the Lower Siwalik of the Surai Khola section, (B) Multistoried sandstones interbedded with mudstone beds in the Middle Siwalik of the Karnali River section, (C) Conglomerate units interbedded with mudstones in the Upper Siwalik of the Surai Khola section, and (D) A mudstone sampling site in the Lower Siwalik of the Surai Khola section (hammer is 28 cm in length).

Detailed paleomagnetic ages for the Siwalik sediments are available for different river sections of Nepal (e.g., Appel et al., 1991; Gautam and Rösler, 1999; Gautam and Fujiwara, 2000; Ojha et al., 2009). For this study, we selected two river sections, the Karnali River section

strata ranging in age from 16 Ma to 5.2 Ma (Gautam and Fujuiwara, 2000), and the Surai Khola section representing strata 13 Ma to 2 Ma (Appel et al., 1991).

Materials and methods

Mudstone and some paleosol samples (n = 49) were collected with an average sampling interval of 0.25 to 0.5 Myr from both the Karnali River and the Surai Khola sections. Well constrained paleomagentic age data for the sedimentary succession along the both river sections have been completed by previous researchers (e.g., Appel et al., 1991; Gautam and Rösler, 1999; Gautam and Fujiwara, 2000). The sample processing and chemical analysis including CSIA were performed in the organic geochemistry laboratory at Brown University, Rhode Island, USA following the procedures detailed in Liu et al. (2005) and Gao et al. (2011).

The sedimentary samples were freeze-dried for 12 hours and grinded to fine size. The organic materials in the powdered sample were extracted using an ASE 200 (Accelerated Solvent Extractor) with a mixture of dichloromethane DCM and methanol (9:1) at 120° C and 1200 psi. The extracts were dried under nitrogen gas and passed through a silica-based LC-NH_2 column using a mixture of DCM/isoproponal (2:1) and ethyl ether/acetic acid (96:4) to separate neutral and acid fractions, respectively. The extracted neutral fraction was further eluted in a silica gel column (LC-SiO_2) by a hexane solution to obtain *n*-alkanes. Further cleanup of the acid fraction was performed by mixing it with a mixture of acetyl chloride/cold methanol (5:95) and overnight heating at 60° C. The fatty acid methyl esters was recovered by adding ~ 3ml of 5% NaCl water solution and hexane. Likewise, the obtained fatty acid further refined with DCM by passing through silica gel for one more time. Finally, the *n*-alkane and *n*-alkonic acid extracts were run to the gas chromatograph fame ionization detector (GC-FID) to check the concentration of organic compounds in the prepared sample.

Identification of specific *n*-alkyl (*n*-alkane and *n*-alkonic acid) compounds was based on comparison of mass spectra from GC-MS (Gas Chromatography-Mass Spectrometry) with respect to GC retention times (Gao et al., 2011). Finally, organic compounds (*n*-alkyl) were run in a HPLC-MS to obtain compound specific δD values and $\delta^{13}C$ values. In this study, we targeted long-chain odd and even number compounds that are originally derived from the terrestrial higher plants. The odd number compounds (C_{27} to C_{31}) from the *n*-alkane fraction are used for $\delta^{13}C$ study and *n*-alkane compounds C_{27} and C_{29} are used for the δD study (Fig. 3.3, 3.4). However, due to low concentration of *n*-alkanes, *n*-alkonic acid compounds (C_{26} and C_{28}) are used for δD study in the Karnali River section.

For the GDGT sample preparation, the neutral fraction of organic compounds were eluted in silica gel column (LC-SiO_2) with hexane, dichloromethane (DCM) and methanol (MeOH). The methanol fraction was serially eluted further through Al_2O_3 column with hexane:DCM (9:1) and a mixture of hexane:DCM (1:1) and DCM:MeOH (1:1) and blown out completely with the help of nitrogen gas. The DCM:MeOH fraction of organic compounds was dissolved in a solution of hexane: isopropanol (99:1) and passed through a 0.2 µm filter. The final extract was analyzed with a HPLC-MS.

GDGTs are large membrane lipid generally produced by Archaea and some bacteria commonly found in lake, soils and oceans (Tierney, 2012). There are two types of GDGTs (isoGDGTs and brGDGTs). Where brGDGTs are commonly found in soils, peats, lakes, and marginal environments (Tierney, 2012) but not in the pelagic marine environments (Hopmans et al., 2004). As our study deals with floodplain deposits, we applied brGDGTs as a temperature proxy. The production of GDGT is sensitive to soil temperature, and can be used to calculate MAAT (Weigers et. al., 2007). Temperatures are calculated using both methods described by

Weijers et al. (2007) and Peterse et al. (2012). Although both methods produced similar values (Fig. 3.5), our paleotemperature interpretation is based on the recent procedure of Peterse et al. (2012).

Results:

Surai Khola section:

A total of 20 samples were analyzed from this section. The carbon isotope ($\delta^{13}C$) values of *n*-alkane C_{27}, C_{29} and C_{31} are strongly correlated to each other (Fig. 3.3), and we used the value of C_{27} for vegetation change interpretation. The $\delta^{13}C$ values range from –32.33‰ at 10 Ma to –18.67‰ at 3.85 Ma (Table 3.1). From 12 to 5.5 Ma, the $\delta^{13}C$ values show a minor enriching trend in general. Around 5.5 Ma, $\delta^{13}C$ started to enrich conspicuously. From 3.5 to 2.5 Ma, the $\delta^{13}C$ values show a greater variability with a major enrichment trend (Fig. 3.6).

The δD values obtained from *n*-alkane C_{27} and C_{29} are strongly correlated with each other (Fig. 3.4C), and we use the value of C_{27} for our interpretation. The δD values ranges from -106.19‰ to -180.58‰ with an average of -143.38‰ (Table 3.2). From 12 to 3.85 Ma, the maximum depletion of δD occurred around 10 Ma and 3.85 Ma, whereas the maximum enrichment occurred around 9 Ma (Fig. 3.6A). From 12 Ma to 5.5 Ma, δD values show a cyclic pattern, but from 5.5 Ma to 3.8 Ma, δD values remain depleted highly. Overall δD values show a general depletion trend from 12 Ma to 3.8 Ma.

The GDGT values in the Surai Khola section were obtained from 11.20 Ma to 2.5 Ma age range. Although the values of mean annual air temperature (MAAT) calculated with approaches of Weijers et al. (2007) and Peterse et al. (2012) are strongly correlated with each other (Fig. 3.5A), we used MAAT values obtained with Peterse et al. (2012) method. Paleotemperatures in

the Surai Khola section range from 13.5 °C to 23.5 °C with the average of 18 °C (Table 3.3). Paleotemperature data show the lowest value of 13.5 °C at 11.2 Ma and the highest value of 23.5 °C at 3 Ma. Temperature pattern shows a cyclic change from 12 Ma to 5.5 Ma, after which it remained high (Fig. 3.6A). From 12 to 2.5 Ma, temperature values show an overall increase trend. Around 5.5 Ma, temperature started to increase conspicuously with a breakdown of the cyclical changing pattern (Fig. 3.6A).

Table 3.1. $\delta^{13}C$ values of *n*-alkane C_{27}, C_{29} and C_{31} for the Surai Khola samples.

		$\delta^{13}C$ *n*-alkane (‰)		
Sample #	Age (Ma)	C_{27}	C_{29}	C_{31}
13-NP-SK-29	2.50	-19.09	-19.72	-18.95
13-NP-SK-30	3.00	-24.55	-26.79	-24.87
12-NP-SK-26	3.85	-18.67	-18.96	-18.66
12-NP-SK-25	4.70	-26.22	-28.12	-25.27
12-NP-SK-24	5.20	-23.64	-25.62	-25.96
12-NP-SK-16	5.40	-26.96	-26.84	-33.92
12-NP-SK-15	5.55	-26.76	-25.65	-23.34
12-NP-SK-14	6.05	-28.34	-27.22	-25.31
12-NP-SK-13	6.50	-29.51	-30.39	-31.77
12-NP-SK-11	7.00	-29.78	-30.01	-29.33
12-NP-SK-10	7.50	-29.75	-30.56	-31.18
12-NP-SK-9	8.00	-30.08	-30.05	-29.89
12-NP-SK-7	8.50	-31.14	-31.45	-32.59
12-NP-SK-5	9.00	-30.10	-30.47	-32.42
12-NP-SK-4	9.50	-30.53	-30.68	-31.76
12-NP-SK-2	10.00	-32.33	-32.95	-34.31
12-NP-SK-23	10.80	-28.03	-29.21	-31.80
12-NP-SK-22	11.20	-30.44	-30.76	-31.89
12-NP-SK-20	11.95	-29.19	-29.21	-30.45

Table 3.2. δD values measured in *n*-alkane C_{27} and C_{29} in the Surai Khola section

		δD *n*-alkane fraction (‰)	
Sample #.	Age (Ma)	C_{27}	C_{29}
12-NP-Sk-29	2.50	-----	-----
12-NP-Sk-30	3.00	-----	-----
12-NP-Sk-26	3.85	-180.58	-194.52
12-NP-Sk-25	4.70	-179.59	-191.71
12-NP-Sk-24	5.20	-157.80	-165.89
12-NP-Sk-16	5.40	-172.13	-189.63
12-NP-Sk-15	5.55	-136.03	-154.34
12-NP-Sk-14	6.05	-118.34	-133.65
12-NP-Sk-13	6.50	-156.60	-174.74
12-NP-Sk-11	7.00	-159.72	-163.07
12-NP-Sk-10	7.50	-118.74	-122.15
12-NP-Sk-9	8.00	-147.27	-143.62
12-NP-Sk-7	8.50	-129.76	-136.59
12-NP-Sk-5	9.00	-106.19	-139.42
12-NP-Sk-4	9.50	-126.99	-136.78
12-NP-Sk-2	10.00	-186.05	-184.14
12-NP-Sk-1	10.40	-----	-----
12-NP-Sk-23	10.80	-121.38	-135.92
12-NP-Sk-23a	10.80	-118.90	-134.70
12-NP-Sk-22	11.20	-148.52	-152.34
12-NP-Sk-20	11.95	-113.48	-133.01

Table 3.3. Paleotemperature values for the Surai Khola section.

		Based on Weijer et al. (2007)	Based on Peterse et al.(2012)
Sample #:	Age (Ma)	MAAT (°C)	MAAT (°C)
12-NP-SK-29	2.50	18.9	17.5
12-NP-SK-30	3.00	28.2	23.5
12-NP-SK-26	3.85	26.3	18.8
12-NP-SK-25	4.70	25.8	18.8
12-NP-SK-24	5.20	24.6	17.9
12-NP-SK-16	5.40	18.5	14.5
12-NP-SK-15	5.55	30.7	22.2
12-NP-SK-14	6.05	24.6	15.3
12-NP-SK-13	6.50	17.3	14.2
12-NP-SK-11	7.00	28.0	20.6
12-NP-SK-10	7.50	27.7	19.3
12-NP-SK-9	8.00	24.1	16.7
12-NP-SK-7	8.50	21.0	16.3
12-NP-SK-5	9.00	27.8	18.4
12-NP-SK-4	9.50	24.9	17.8
12-NP-SK-23a	10.80	26.7	20.0
12-NP-SK-22	11.20	17.4	13.5
12-NP-SK-20	11.95	-----	-----

MAAT: mean annual air temperature

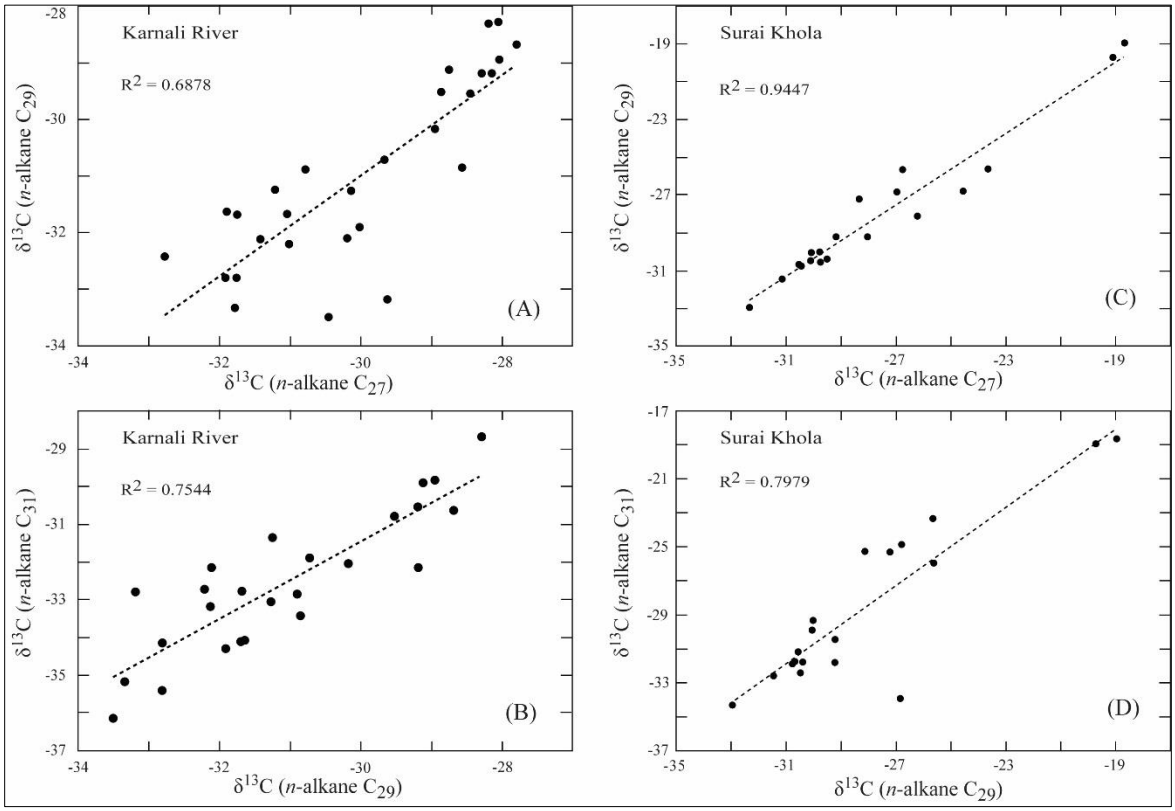

Figure 3.3. Correlations between $\delta^{13}C$ of C_{27} and $\delta^{13}C$ of C_{29} (A and C), and $\delta^{13}C$ of C_{29} and $\delta^{13}C$ of C_{31} (B and D) for both the Karnali River (A and B) and Surai Khola sections (C and D).

Karnali River section:

In the Karnali River section, a total of 29 samples were analyzed for the isotopic study. Paleomagnetic ages of these samples range from 16 Ma to 5.2 Ma. $\delta^{13}C$ values of the *n*-alkanes (e.g., C_{27}, C_{29} and C_{31}) are strongly correlated with each other (Fig. 3.3A, B), and we have chosen C_{27} values for data interpretation. $\delta^{13}C$ values in the Karnali River section (Table 3.4) range from -27.80‰ to -32.78‰ with an average of -29.98‰ (Table. 3.4). Between 16 to 14.5 Ma, $\delta^{13}C$ values slightly depleted from -29.63‰ to -31.22‰, but enriched by ~3‰ at 14 Ma and remained fairly the same until 9.5 Ma. From 9.5 Ma to 5.25 Ma, $\delta^{13}C$ values show some variabilities with higher depleted values of ~ -31‰ at 8.75, 7.25 Ma, and ca. 6 Ma, and the highest depletion of ~ -33‰ at 5.25 Ma (Fig. 3.6B). Meanwhile, during the intervening enriching

period, $\delta^{13}C$ values enriched to -28.96‰ at 7.75 Ma, and to ~ -28‰ between 6.5 and 7 Ma (Fig. 3.6B). In general, $\delta^{13}C$ values show a slight depleting trend over time.

Table 3.4. $\delta^{13}C$ values of *n*-alkane C_{27}, C_{29} and C_{31} for the Karnali River samples.

		$\delta^{13}C$ *n*-alkane (‰)		
Sample #:	Age (Ma)	C_{27}	C_{29}	C_{31}
13-NP-KR-50	5.20	-30.02	-31.91	-34.30
13-NP-KR-49	5.25	-32.78	-32.43	-46.33
13-NP-KR-48	5.50	-30.46	-33.50	-36.14
13-NP-KR-47	5.90	-31.92	-32.80	-34.15
13-NP-KR-46	6.00	-31.79	-33.34	-35.19
13-NP-KR-44	6.25	-31.90	-31.64	-34.08
13-NP-KR-43	6.40	-28.57	-30.85	-33.43
13-NP-KR-42	7.00	-28.15	-29.19	-30.54
13-NP-KR-41	7.25	-31.76	-32.81	-35.41
13-NP-KR-40	7.50	-31.43	-32.12	-33.18
13-NP-KR-39	7.75	-28.96	-30.17	-32.03
13-NP-KR-38	8.00	-29.67	-30.72	-31.89
13-NP-KR-37	8.25	-30.79	-30.90	-32.85
13-NP-KR-36	8.50	-31.05	-31.68	-32.76
13-NP-KR-35	8.75	-31.75	-31.69	-34.11
13-NP-KR-34	9.00	-30.14	-31.27	-33.05
13-NP-KR-32	9.50	-28.04	-28.95	-29.83
13-NP-KR-29	10.25	-27.80	-28.68	-30.63
13-NP-KR-28	10.50	-28.06	-28.28	-28.68
13-NP-KR-25	11.25	-28.30	-29.18	-32.15
13-NP-KR-22	12.00	-28.87	-29.52	-30.78
13-NP-KRa-22	13.00	-28.46	-29.54	----
13-NP-KRa-20	13.50	-28.20	-28.31	----
13-NP-KR-18	14.00	-28.76	-29.12	-29.90
13-NP-KR-16	14.50	-31.22	-31.25	-31.36
13-NP-KR-14	15.00	-31.02	-32.21	-32.72
13-NP-KR-13	15.40	-30.19	-32.11	-32.15
13-NP-KR-11	16.00	-29.63	-33.19	-32.79

Table 3.5. δD values of *n*-alkonic acid C_{24}, C_{26}, and C_{28} in the Karnali River section

		δD acid fraction (‰)		
Sample #:	Age (Ma)	C_{24}	C_{26}	C_{28}
13-NP-KR-50	5.20	-174.88	-179.06	-198.09
13-NP-KR-49	5.25	-166.26	-164.80	-175.49
13-NP-KR-48	5.50	-187.25	-188.60	-193.68
13-NP-KR-47	5.90	-165.73	-171.22	-187.77
13-NP-KR-46	6.00	-164.30	-166.69	-169.68
13-NP-KR-44	6.25	-175.22	-173.37	-180.14
13-NP-KR-43	6.40	-172.60	-167.40	-193.59
13-NP-KR-45	6.75	-----	-----	-153.48
13-NP-KR-42	7.00	-----	-----	-153.50
13-NP-KR-41	7.25	-166.82	-176.11	-176.22
13-NP-KR-40	7.50	-168.40	-166.70	-----
13-NP-KR-39	7.75	-----	-----	-150.01
13-NP-KR-38	8.00	-163.98	-167.20	-179.02
13-NP-KR-37	8.25	-173.46	-166.31	-162.91
13-NP-KR-36	8.50	-152.01	-154.34	-168.74
13-NP-KR-34	9.00	-160.02	-156.84	-164.94
13-NP-KR-22	12.00	-----	-121.70	-----
13-NP-KR-11	16.00	-----	-143.89	-161.32

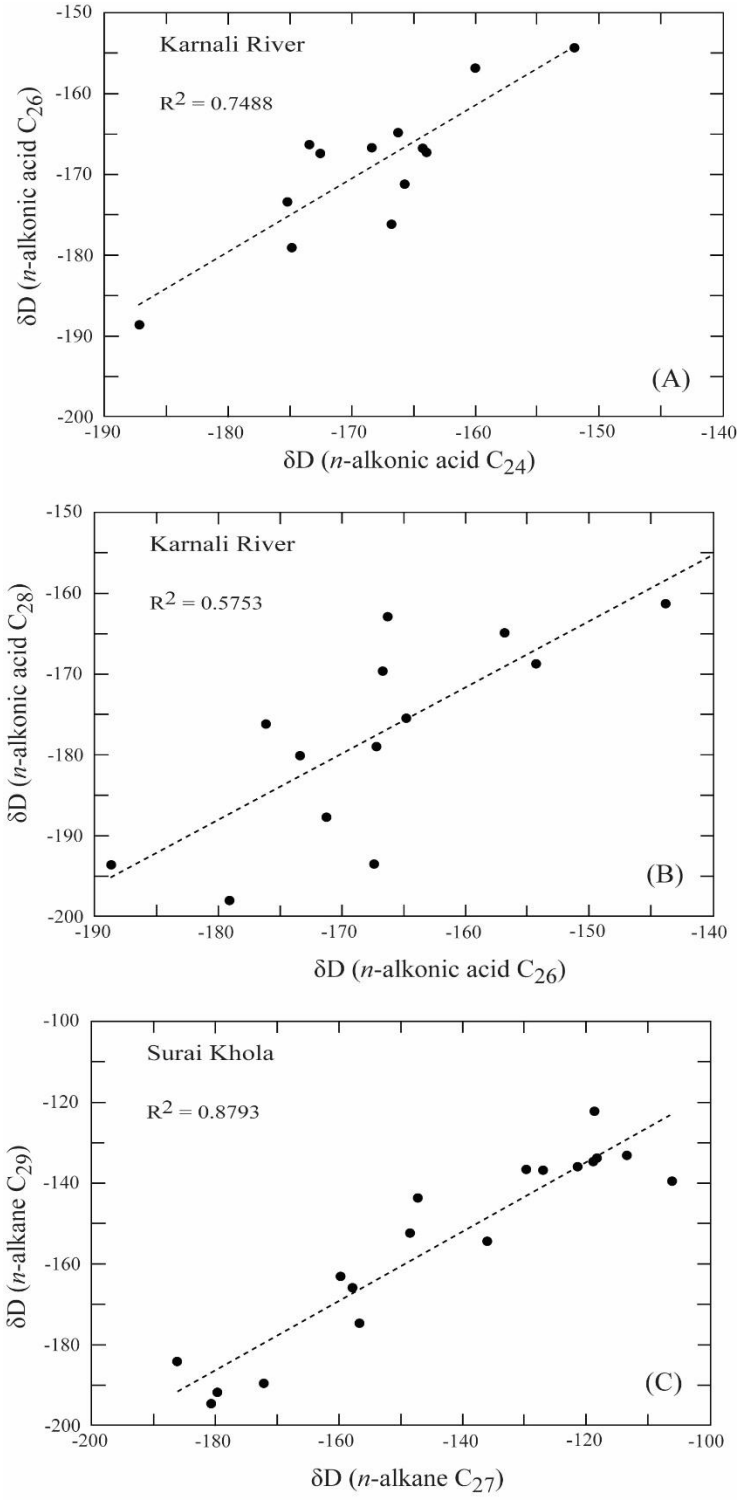

Figure 3.4. (A) and (B) Correlations of δD values for C_{24} vs. C_{26} and C_{26} vs. C_{28} for the Karnali River section, and (C) Correlation of δD values for C_{27} vs. C_{29} for the Surai Khola section.

Due to the low concentration of lipid biomarker, we were unable to obtain δD values from *n*-alkane fraction. However, we present the δD result obtained from the *n*-alkonic acid fraction in Table 3.5. Even in *n*-alkonic fraction, there is data gap between 16 to 12 Ma and 12 to 9 Ma. δD values obtained from *n*-alkonic acids of C_{24}, C_{26} and C_{28} strongly correlate to each other (Fig. 3.4A and B), and we based our interpretation on C_{28} values. δD values show cyclical patterns superimposed on an overall depleting trend with time. δD values range from -150.01‰ to -198.09‰ with an average value of -173.04‰. Greater enrichments are observed at 7.75, 7 and 6.75 Ma with a value of ~ -152‰. Whereas, the highest depletion is observed at 5.2 Ma with a value of -198.09‰. Because of the lack of age data < 5.2 Ma, we are unable to present δD values for younger rocks.

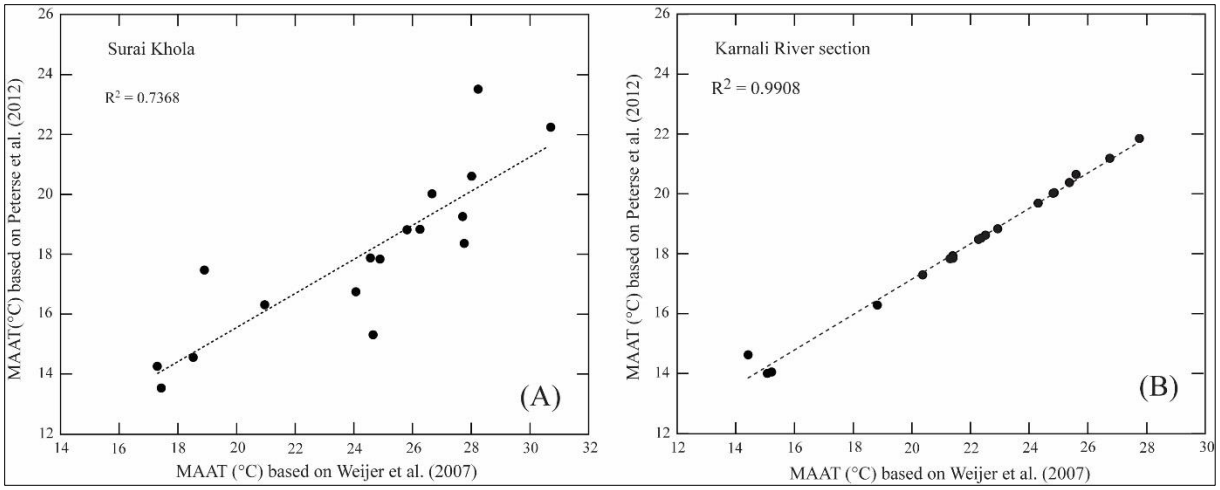

Figure 3.5. Correlation of paleotemperature values (MAAT: mean annual air temperature in °C) calculated based on Weijer et al. (2007) versus Peterse et al. (2012) for both Surai Khola (A) and Karnali River (B) sections.

GDGT data for the Karnali River section range from 16 Ma to 5.2 Ma (Table 3.6). The temperature values range from 14 °C to 21.8 °C with an average of ~18 °C. From 15.4 to 12 Ma temperature remained fairly constant (~18 °C) but dropped to a minimum of 14 °C at 11.25 Ma. Since 11.25 Ma, temperature gradually increased to 19.7 °C at 8.5 Ma and then decreased to 14.1 °C at 8.25 Ma. Since 8.25 Ma, temperature increased to 21.8 °C (maximum) at 7.75 Ma and then

dropped to 14.6 °C at 6.4 Ma. Since 6.4 Ma, temperature continuously increased to 20.6 °C at 5.2 Ma with an exception of a minor fall to 17.3 °C at 5.5 Ma (Fig. 3.6B).

.

Table 3.6. Paleotemperature values for the Karnali River Section.

		Based on Weijer et al. (2007)	Based on Peterse et al. (2012)
Sample #:.	Age (Ma)	MAAT (°C)	MAAT (°C)
13-NP-KR-50	5.20	25.6	20.6
13-NP-KR-49	5.25	24.8	20.0
13-NP-KR-48	5.50	20.4	17.3
13-NP-KR-47	5.90	22.5	18.6
13-NP-KR-46	6.00	24.8	20.0
13-NP-KR-44	6.25	22.3	18.5
13-NP-KR-43	6.40	14.4	14.6
13-NP-KR-41	7.25	26.7	21.2
13-NP-KR-40	7.50	25.4	20.4
13-NP-KR-39	7.75	27.7	21.8
13-NP-KR-38	8.00	18.8	16.3
13-NP-KR-37	8.25	15.2	14.1
13-NP-KR-36	8.50	24.3	19.7
13-NP-KR-34	9.00	21.3	17.8
13-NP-KR-32	9.50	21.3	17.8
13-NP-KR-25	11.25	15.1	14.0
13-NP-KR-22	12.00	21.4	17.9
13-NP-KRa-22	13.00	22.4	18.5
13-NP-KR-13	15.40	21.4	17.9
13-NP-KR-11	16.00	22.9	18.8

MAAT: mean annual air temperature

Discussion:

Carbon isotope (vegetation proxy):

Some previous $\delta^{13}C$ isotopic studies of the Siwalik strata (e.g., Quade and Cerling, 1995; Quade et al., 1995; Behrensmeyer et al., 2007; Sanyal et al., 2010) suggested different phases of vegetation shift (from C_3 forest to C_4 grassland) in the Himalayan foreland. Our isotopic study using lipid biomarker extracted from the flood plain deposits revealed new insight of the Neogene vegetation shift in the region. Using $\delta^{13}C$ of pedogenic carbonate, Quade et al. (1995) suggested a dramatic expansion of C_4 vegetation around 7 Ma in the Surai Khola section. However, our $\delta^{13}C$ values for the same section obtained from *n*-alkane C_{27} show that the expansion of C_4 vegetation likely started earlier at ca. 8.5 Ma, gained a faster transition around 6.5 Ma, and become dominant around 5.5 Ma (Table 3.1, Fig. 3.6A).

However, the $\delta^{13}C$ values of *n*-alkane C_{27} from the Karnali River section do not show any clear trend like that of the Surai Khola section (Table 3.4; Fig. 3.6B). From 16 Ma to 5.2 Ma, where 5.2 Ma represent the youngest sample in the section, no clear signal of vegetation change can be seen. Although there may be a partial appearance of C_4 vegetation from 14 to 9.5 Ma (Fig. 3.6B), the area was likely dominated by C_3 plants between 9.5 and 5.2 Ma, contradicting the results of the Surai Khola section where a gradual expansion of C_4 vegetation with time is clear (Fig. 3.6A). We speculate that, such an asynchronous pattern of C_3 vegetation expansion in the younger succession of the Karnali River section likely linked to the existence of a riparian vegetation in the Neogene floodplain along the paleo-Karnali River.

As documented in previous studies about a heterogeneous expansion of C_4 vegetation in the Neogene Siwalik succession in Pakistan and India (Quade and Cerling, 1995; Quade et al.,

1995; Sanyal et al., 2004, 2005, 2010), the present study not only revealed a gradual expansion of C_4 vegetation but also showed that the vegetation expansion can be heterogeneous within a short lateral distance of 200 km. In Pakistan, the expansion of C_4 vegetation occurred at 7.7 Ma (Quade and Cerling, 1995), and in the Indian sections of Siwalik, the transition from C_3 to C_4 plants occurred between 9 and 6 Ma (Sanyal et al., 2004, 2005, 2010). Our study shows that such transition started at 8.5 Ma and completed by 5.2 Ma in the Surai Khola section, but no dominant C_4 signal was detected in the Karnali River section at least till 5.2 Ma (Fig. 3.6B). This asynchronous pattern of vegetation shift within the entire ~2000 km long Neogene foreland basin indicates that microscale (i.e., local scale) climate dynamics likely influenced the vegetation shift. Local influences, like seasonality, forest fires, and rainfall amount, are thought to be the causes for such heterogeneities in the vegetation shift (Tipple and Pagani, 2007).

Hydrogen isotopes (precipitation proxy):

As described by Dansgaard (1964) depletion of rainwater δD (and $\delta^{18}O$) is associated with the "amount effect" such that the higher the rainfall amount the greater the depleted (i.e., negative) isotope values. A similar relation between rainfall amount and rainwater isotope values was also reported in New Delhi, India (e.g., IAEA, 2003; Bhattacharya et al., 2003). The hydrogen isotope data of lipid biomarkers from both the Surai Khola (C_{27} of *n*-alkane) and Karnali River (C_{28} of *n*-alkonic acid) sections (Table 3.2 and Table 3.5) show a cyclic variability in rainfall amount. The results of the Surai Khola section show a greater depletion of δD values at 10 Ma (-186.05‰), indicating a wetter period (Fig. 3.6A). Around 5.5 Ma, the cyclic trend breaks down with a heavier depletion of δD thus a significant increase in rainfall. In both river sections, rainfall increase with time in general.

A previous study (Quade et al., 1995) in the Surai Khola section showed that the enrichment of pedogenic $\delta^{18}O$ started since 6 Ma. However, in the Quade and Cerling (1995) study, such trend of decreasing rainfall was suggested to start 2 myr early in Pakistani Siwalik. In contrast, our δD values of *n*-alkane C_{29} of the Surai Khola section shifted in opposite trend, i.e., they gradually depleted (increasing rainfall) with time with major depletion around 5.5 Ma (Fig. 3.6A). $\delta^{18}O$ in soil carbonate and δD in clay minerals from the Indian Siwalik along the Haripur Khola (Fig. 3.1A), west of the Yamuna River, showed high rainfall activity around 4 Ma (Ghosh et al., 2004). Sanyal et al. (2010) proposed two occurrences of monsoon intensifications (increasing or decreasing annual rainfall?) at around 3 and 6 Ma, based on the δD values of clay minerals from the same area. Furthermore, based on the $\delta^{18}O$ results of soil carbonates, they proposed two additional phases of monsoon intensifications around 11 and 6 Ma in the Kangra Valley area. Likewise, further west in Jammu area (Fig. 3.1A) of the Indian Siwalik, Singh et al. (2012) proposed three phases of rainfall intensifications (so-called monsoon intensification?) at around 10, 5 and 1.8 Ma based on the $\delta^{18}O$ from pedogenic carbonate. Although the present study indicates two phases of rainfall intensifications at 10 Ma and 5.5 Ma in the Surai Khola section the most intriguing part is the overall trend of the rainfall. Most previous studies showed an enrichment (i.e., less rainfall) of δD and $\delta^{18}O$ values with time. In contrast, our results showed an opposite trend, i.e., depletion of δD values thus increasing rainfall with time (Fig. 6). Our results also contradict with the results reported in Clift et al. (2008), where the chemical weathering study of sediment cores, (ODP 718, Bengal fan), exhumation rate ($^{40}Ar/^{39}Ar$ muscovite thermochronology) from the Himalayan hinterland and proximal foreland, and the sedimentation rate in the (Indus fan suggest decreasing rainfall trend until ca. 3.5 Ma.

Such an asynchronous pattern of rainfall intensification within short lateral distances along the Siwalik Range in Pakistan, India and Nepal could be related to local topographic changes, which can be linked with the spatio-temporal variability of tectonic uplift of the Himalaya by imbrication, activation, and reactivation of the major thrust faults (e.g., MCT and MBT) between 12 to 10 Ma and around 6 Ma in Central Himalaya (Huyghe et al., 2001; Catlos et al., 2002). Similarly, the increasing rates of sedimentation and the development of multistory channel sandbodies in the Siwalik, especially in the Karnali River section (Huyghe et al., 2005), between 6.5 and 5.5 Ma support of the presence of local changes of river discharge thus rainfall in the Neogene foreland basin.

GDGTs (Temperature Proxy):

The paleo-temperature results (Table 3.3) for the Surai Khola section indicate periodic fluctuation between 12 Ma and 5.5 Ma (Fig. 3.6), whereas since 5.5 Ma the temperature gradually increased and reached a maximum of 23.5 °C at 3 Ma. The overall trend of paleotemperature in this section is slightly increasing with time, with an average temperature of 18 °C for the study interval. Similarly, data for the Karnali River section (Table 3.6) reveal a variability in temperature between 16 and 5.2 Ma. Similar to that of the Surai Khola section, paleo-temperature in the Karnali River section increases with time, resulting a similar average temperature (~ 18 °C).

Integration of all results ($\delta^{13}C$, δD and GDGT):

The δD and temperature values from both river sections show negative correlation until 5.5 Ma, suggesting that the amount of rainfall was higher during low temperature period and the amount of rainfall was lower during high temperature period (Fig. 3.6A, B). However, the modern monsoon patterns in the Indian subcontinent shows a positive correlation between

rainfall and temperature, i.e., higher amount of rainfall during warmer time (in the summer) between June to September and little rainfall during cooler time (in the winter) between December to February (Gupta, 2010; Gupta et al., 2015). This seasonal rainfall is fully depended on the wind circulation pattern: the summer monsoon is due the low-latitude southwesterly wind coming from the Bay of Bengal and Arabian Sea, whereas the winter monsoon is due to the northeasterly wind coming from the Asian interior (Schott and McCreary, 2001; Kuppusamy and Ghosh, 2012).

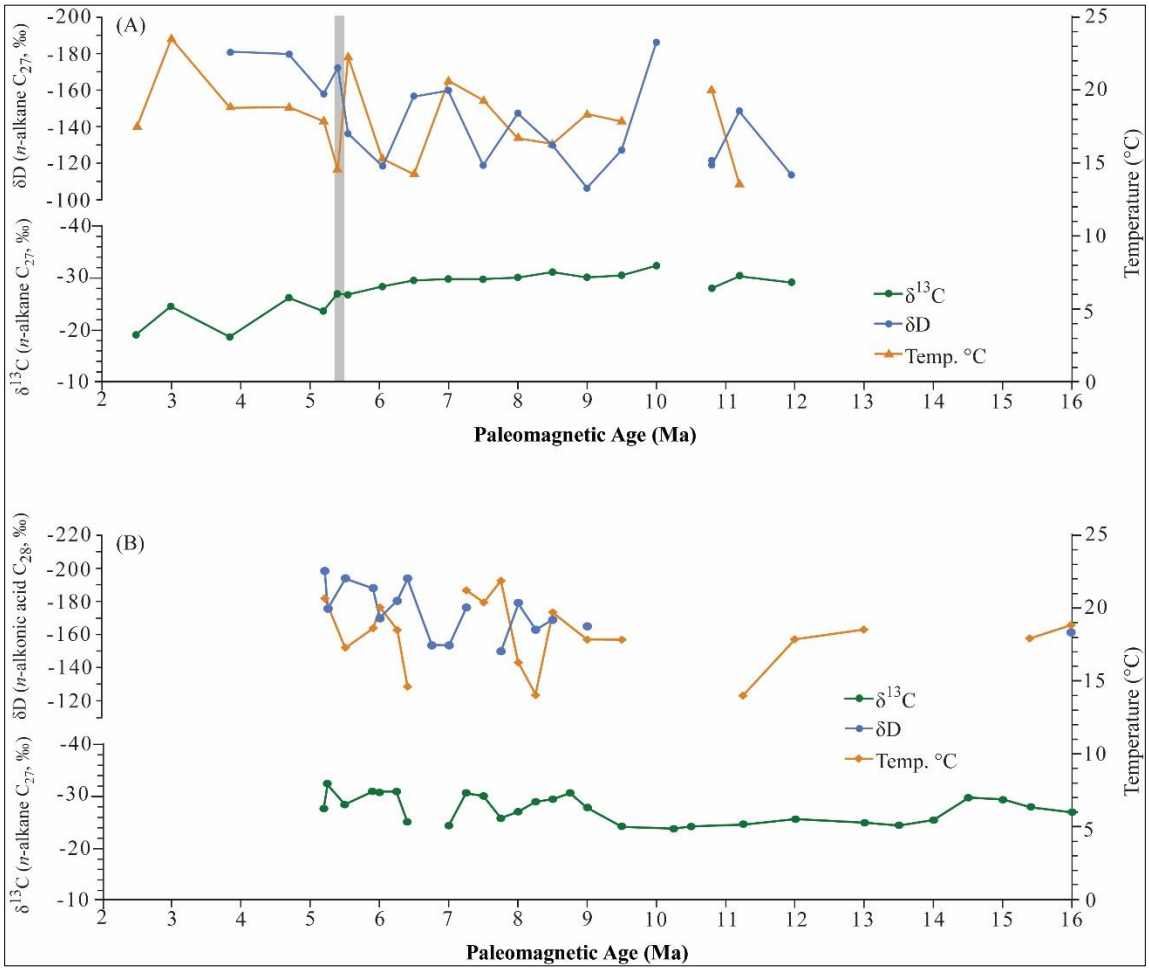

Figure 3.6. Correlation between $\delta^{13}C$, δD and GDGT-based paleotemperature for the Surai Khola section (A) and the Karnali River section (B). The shaded line represents the onset of Indian monsoon and the vegetation shift. Paleomagnetic dates are from Appel et al. (1991) and Gautam and Fujiwara. (2000).

Some previous studies linked the Indian monsoon initiation/intensification to the Tibetan Plateau uplift, critical height gain by the Himalayas, and solar radiation (Quade et al., 1989; Ruddiman and Kutzbach, 1989; Prell and Kutzbach, 1992). The equilibrium sensitivity coefficient (ESC) modeling indicated the Himalayan-Tibetan Plateau must have been less than half the current height prior to 8 Ma (Prella nd Kutzbach, 1992; Prell et al., 1992). Recently, Gupta et al. (2015), based on the data of the ocean drilling program (ODP Hole 722B, 728B, 730A, and 731A) at Oman margin, suggested the presence of a weaker summer monsoon winds in the region between 11 to 7 Ma when Findlater jet was either weak or its axis was positioned far away from Oman margin Hole 730A. They also emphasized the presence of a stronger winter monsoon based on the high percentage of *G. bulloides* at the Owen Ridge Hole 731A. Thus, they argued that the higher sedimentation rate during 11 to 7 Ma, previously reported by Sangode and Kumar (2003) and Raiverman (2002) in the Himalayan foreland, could be due to the winter precipitation during strong mid-latitude westerlies when the summer monsoon winds were weaker. Notably, the mid westerlies in the northern hemisphere can get stronger and shift southward during the colder geologic time.

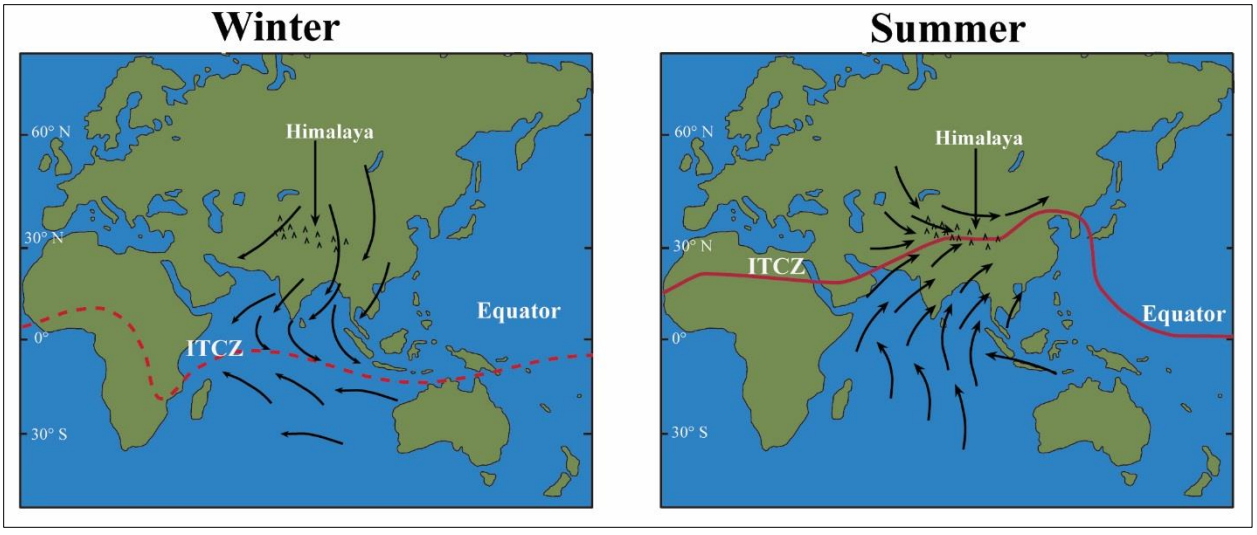

Figure. 3.7. Modern-day wind circulation pattern in South Asia during winter and summer. ITCZ refers to Intertropical Convergence Zone. (Modified after ThoughtCo., 2017).

Our results indicate occurrence of higher rainfall during colder geologic times and lower rainfall during warmer times before 5.5 Ma (Fig. 3.6). As the modern day rainfall pattern in the Indian subcontinent shows higher amount of rainfall during summer than during winter (Fig. 3.7), we propose that the negative correlation between rainfall and mean annual air temperature (MAAT) prior to 5.5 Ma could be related to the strong presence of mid-latitude westerlies in the region, when summer monsoon winds were weaker, that brought enhanced winter-precipitation particularly during colder periods (Fig. 3.8).

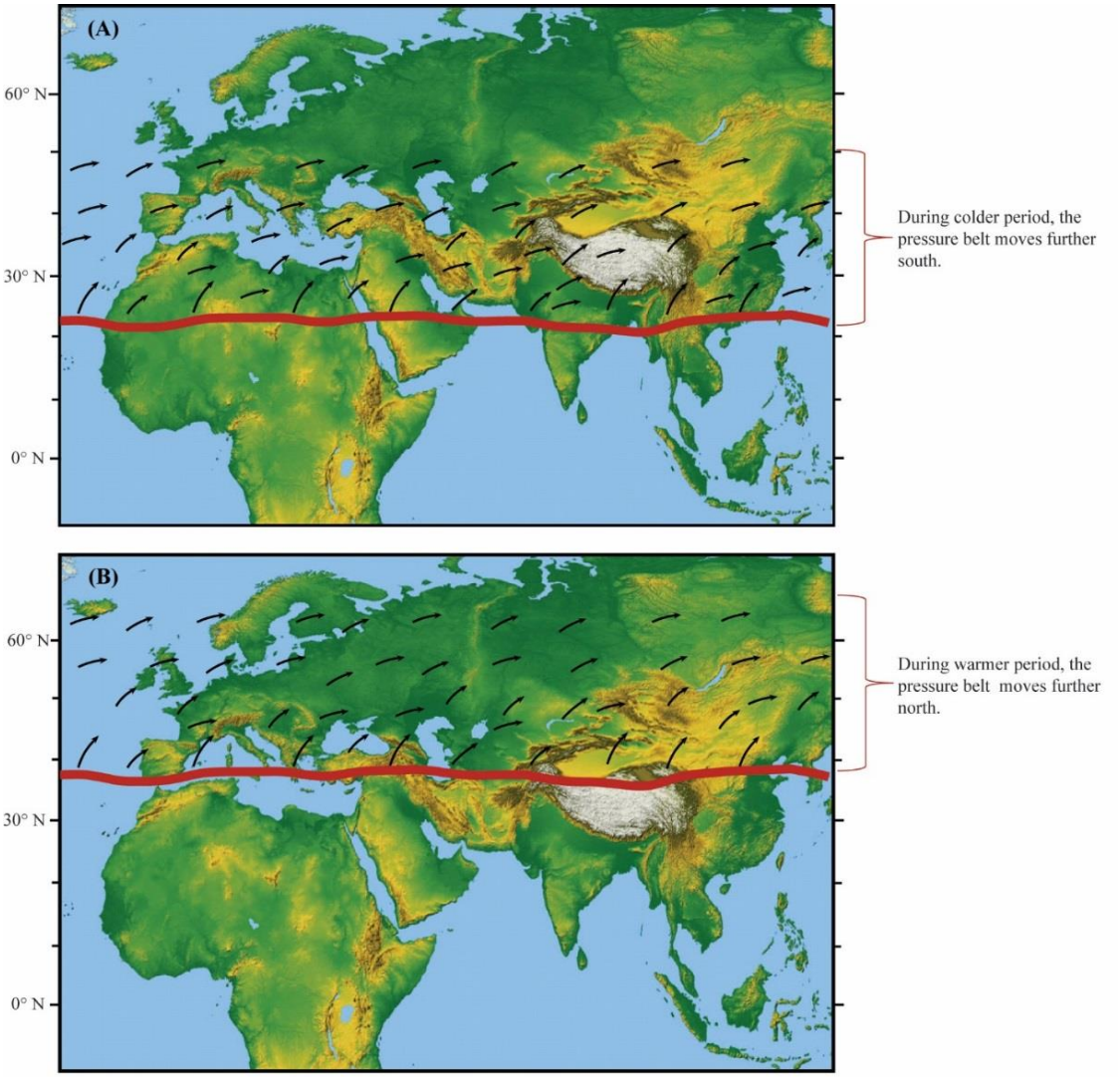

Figure. 3.8. Schematic map representation the wind circulation patter before 5.5 Ma. During colder geological times, mid-latitude pressure belt moved further south and caused more rainfall in the Himalayan front (A), whereas during warmer times, the mid-latitude pressure belt moved further north causing less rainfall in the Himalayan front. (Map retrieved from Thinglink, 2015)

After 5.5 Ma, our data show a conspicuous positive correlation between rainfall and annual temperature, indicating the onset of modern-style seasonality in rainfall in the Indian subcontinent. We suggest that the Himalaya likely reached a critical height around 5.5 Ma, blocking the influence of mid-westerlies and enhancing the strength of the summer monsoon winds (Fig. 3.7). This initiated the famous Indian monsoon at that time, creating a hot-wet summer and cold-dry winter, which favored the dominance of C_4 grasses over C_3 trees starting around 5.5 Ma, as reflected in drastic enrichment of $\delta^{13}C$ values around 5.5 Ma in the Surai Khola section (Fig. 3.6A).

Conclusions:

The mudstone and some paleosol samples collected from the Neogene foreland basin strata along the Surai Khola and Karnali River sections of Nepal were chemically analyzed to understand paleoclimatic and paleoechological changes in the region. Our $\delta^{13}C$ results from *n*-alkane C_{27} demonstrate a gradual expansion of C_4 grasses starting at 8.5 Ma and a domination of these plants around 5.5 Ma in the Surai Khola section. However, no clear evidence of the vegetation shift was observed in the Karnali River section.

δD results revealed two phases of rainfall intensifications in the Surai Khola section, one at 10 Ma and the other around 5.5 Ma, with a gradual intensification over time. However, δD data indicate one phase of rainfall intensification in the Karnali River section at 6.5 Ma. Such asynchronous pattern of rainfall and the vegetation change along tectonic strike could be due to the spatio-temporal variability of tectonic uplift of the Himalaya by imbrication, activation, and reactivation of the major thrust faults (MCT and MBT). Moreover, contrary to many previous studies, our δD values demonstrate a gradual increase in rainfall over time.

The negative correlation between temperature and precipitation prior to 5.5 Ma is likely due to the absence of strong summer monsoon before 5.5 Ma when mid-latitude westerlies could freely pass across the subdued Himalaya. Once monsoon started around 5.5 Ma, the vegetation started to shift from C_3 trees to C_4 grasses favored by wet and humid summer and dry and cool winter.

To understand local to regional scale variability in paleohydrology and paleoecology as well as their link to tectonic uplift of the Himalaya, further extensive study is needed along the Siwalik range.

Chapter 4

Conclusions and Future works

Conclusions:

A total of 49 mudstone and some paleosol samples were collected from the paleomagnetically age-constrained Neogene Siwalik strata at the Surai Khola section (from 12 to 2.5 Ma, *n-20*) and the Karnali River section (from 16 to 5.2 Ma, *n=29*). All the samples were chemically analyzed to understand paleoclimate and paleoecological changes in the Himalayan foreland region. We focused on three climate proxies such as: $\delta^{13}C$ (vegetation proxy), δD (precipitation proxy) and brGDGTs (temperature proxy). $\delta^{13}C$ values obtained from *n*-alkane C_{27} of the Surai Khola section showed gradual expansion of C_4 grasses starting at ca. 8.5 Ma, and a domination of C_4 plants around 5.5 Ma. Although some contribution of C_4 plants were observed between 14 and 9.5 Ma, no significant changes in vegetation was observed till 5.5 Ma in the Karnali River section

The δD values indicate two phases of rainfall intensification at 10 Ma and 5.5 Ma in the Surai Khola section. However, only one phase of rainfall intensification can be observed in the Karnali River section at 6.5 Ma. Such incongruence pattern of rainfall along tectonic-strike could be due to the spatial variability of tectonic uplift linked to imbrication, activation and reactivation of major thrust faults (MCT and MBT) in the Himalaya during Neogene (Huyghe et al., 2001; Catlos et al., 2002). Contrary to the results of the previous studies, our δD values in both river sections show depleting trend over time, representing an overall gradual increase in rainfall during the Neogene.

The integration of δD and GDGT-derived paleotemperature showed negative correlation between rainfall and temperature prior to 5.5 Ma, suggesting the absence of seasonality. After 5.5 Ma, rainfall and temperature showed a positive correlation, suggesting the onset of the South Asian monsoon, which is a favorable climate for C_4 grasses over C_3 trees.

Future works:

The present CSIA study focused on two river sections along the Nepalese Siwalik revealed a possible local-scale climate/ecological change within a short (around 200 km) lateral distance. To understand the lateral variability in paleohydrology and paleoecology along ~ 2000 km long Siwalik belt, future studies should target CSIA study along this belt in Nepal, India and Pakistan. Such an integrated along-strike study can reveal regional-scale Neogene climate changes and can help to understand the uplift and exhumation history of the Himalaya and its impact on such changes.

By providing water for agriculture and recharging groundwater, a source for potable drinking water, the Indian monsoon plays a critical role in the lives of more than 1.5 billion people residing the Indian subcontinent. The cutting-edge techniques and methods used in this study are useful in understanding both the past history and modern dynamics of the Indian monsoon across the region.

References:

Appel, E., Rösler, W., and Corvinus, G., 1991. Magnetostratigraphy of the Miocene-Pleistocene Surai Khola Siwaliks in West Nepal. Geophys. J. Int., p. 105, v. 191–198.

Aitchison, J. C., Ali, J. R., and Davis, A. M., 2007. When and where did India and Asia collide? Jour. Of Geophysical Research. V. 112, doi:10.1029/2006JB004706

Auden, J. B., 1935. Traverses in the Himalaya. Rec. Geol. Surv. India, v. 69(2), pp. 123–167.

Behrensmeyer, A.K, Quade, J., Cerling, T.E., Kappelman, J., Khan, I., Copeland, P., Roe, L., Hicks, J., Stubblefield, P., Willis, B.J., and Latorre, C., 2007. The structure and rate of late Miocene expansion of C4 plants: Evidence from lateral variation in stable isotopes in paleosols of the Siwalik Group, northern Pakistan. GSA Bulletin, v. 119, p. 486–1505.

Bhattacharya, S.K., Froehlich, K., Aggarwal, P.K., Kulkarni, K.M., 2003. Isotopic variation in Indian Monsoon precipitation: records from Bombay and New Delhi. Geophysical Research Letters 30 (24), 11–14.

Burbank, D.W., Beck, R.A. and Mulder, T., 1996. The Himalayan Foreland: Asian Tectonics. Cambridge Univ. Press, p. 149-188.

Cande S. C. and Kent C., 1995. Revised calibration of the geomagnetic polarity timescale for the late Cretaceous and Cenozoic. Journal of Geophysical Research, 100(B4), 6093–6095.

Catlos, E.J., Harrison, T.M., Kohn, M.J., Grove, M., Ryerson, F.J., Manning, C.E., Upreti, B.N., 2001. Geochronologic and thermobarometric constraints on the evolution of the Main Central Thrust. Central Nepal Himalaya. Journal of Geophysical Research 106, 16177–16204.

Catlos, E.J., Harrison, T.M., Manning, C.E., Grove, M., Rai, S.M., Hubbard, M.S., Upreti, B.N., 2002. Records of the evolution of the Himalayan orogen from in situ Th–Pb ion microprobe dating of monazite. Eastern Nepal and western Garhwal. Journal of Asian Earth Sciences 20, 459–479.

Cerling TE, Wang Y, Quade J (1993) Expansion of C4 ecosystems as an indicator of global ecological change in the late Miocene. Nature, v. 361, p. 344-345.

Cerling, T. E., J. M. Harris, B. J. MacFadden, M. G. Leakey, J. Quade, V. Eisenmann, and J. R. Ehleringer. 1997. Global vegetation change through the Miocene-Pliocene boundary. Nature, v. 389, p. 153-158.

Cerling, T.E., Wynn, J.G., Andanje, S.A., Bird, M.I., Korir, D.K., Levin, N.E., Mace, W., Macharia, A.N., Quade, J., and Remien, C.H., 2011. Woody cover and hominin environments in the past 6million years. Nature. V. 476; p. 51-56.

Clift, P. D., Hodges, K.P., Heslop, D., Hannigan, R., Long, H.V., and Calves, G., 2008. Correlation of Himalayan exhumation rates and Asian monsoon intensity. Nature geoscience v.1, p. 875-880.

Collister J. W., Rieley G., Stern B., Eglinton T., Fry B. (1994) Compound specific d13C analyses of leaf lipids from plants with differing carbon dioxide mechanisms. Org. Geochem. V. 21, p. 619–627.

Corrie, S.L., and Khon, M.J., 2011. Metamorphic history of the central Himalaya, Annapurna region, Nepal, and implication for tectonics models. Geol. Soc. Am. Bull., v. 123, p. 1863-1879, doi:10.1130/B30376.1.

Dansgaard, W., 1964. Stable isotope in precipitation. Tellus 16, 436–467.

DeCelles, P.G., Giles, K.A., 1996. Foreland basin systems. Basin Res 8(2):105–123.

DeCelles, P., Gehrels, G., Quade, J., Ojha, T., Kapp, P., Upreti, B., 1998b. Neogene foreland basin deposits, erosional unroofing, and the kinematic history of the Himalayan fold-thrust belt, western Nepal. Geol Soc Am Bull 110(1):2–21.

DeCelles, P.G., Gehrels, G.E., Quade. J., Ojha, T., 1998a. Eocene-early Miocene foreland basin development and the history of Himalayan thrusting, western and central Nepal. Tectonics 17(5):741–765.

Dettman, D.L., Kohn, M.J., Quade, J., Ryerson, F.J., Ojha, T.P., and Hamidullah, S., 2001. Seasonal stable isotope evidence for a strong Asian monsoon throughout the past 10.7 m.y. Geology, v. 29, p. 31 – 34.

Dickinson, W.R., 1985. Interpreting provenance relations from detrital modes of sandstones. Proven Arenites 148:333–361.

Edwards, E.J., Osborne, C.P., Strömberg, C.A.E., Smith, S.A., 2010.The origins of C4 grasslands: Integrating evolutionary and ecosystem science. Science v. 328, p. 587–591.

Eglinton G., and Hamilton R. J., 1967. Leaf epicuticular waxes. Science v. 156, 1322–1335.

Feakins, S.J., Levin, N.E., Liddy, H.M., Sieracki, A., Eglinton, T.I., and Bonnefille, R., 2013. Northeast African vegetation change over 12 m.y. Geology v. 41; p. 295 -298.

Ficken K. J., Li B., Swain D. L., and Eglinton G., 2000. An *n*-alkane proxy for the sedimentary input of submerged/floating freshwater aquatic macrophytes. Organic. Geochemistry. v. 31, p. 745–749.

Fox, D.L., and Koch, P.L., 2004. Carbon and oxygen isotopic variability in Neogene paleosol carbonates: constraints on the evolution of theC4-grasslands of the Great Plains, USA. Science direct, palaeogeography, paleoclimatology, palaeoecology 207p. 305 – 329.

Freeman, K.H., and Colarusso, L.A., 2001. Molecular and isotopic records of C4 grassland expansion in the late Miocene. Geochimica et Cosmochimica Acta, v. 65, p. 1439-1454.

Gansser, A., 1964. Geology of the Himalayas. Interscience Publishers, London.

Gao, L., Hou, J., Toney, J., MacDonald, D., and Huang, Y., 2011. Mathematical modeling of the aquatic macrophyte inputs of mid-chain n-alkyl lipids to lake sediments: Implications for interpreting compound specific hydrogen isotopic records. Science direct Geochimica et Cosmochimica Acta v. 75 p. 3781–3791.

Gautam, P., and Rösler, W., 1999. Depositional Chronology and Fabric of Siwalik Group Sediments in Central Nepal from Magnetostratigraphy and Magnetic Anisotropy. Journal of Asian Earth Sciences, v. 17, p. 659-682.

Gautam, P., and Fujiwara, Y., 2000. Magnetic polarity stratigraphy of Siwalik Group sediments of Karnali River section in Western Nepal. Geophysical Journal International, 142 (3): 812–824.

Gautam P., Hosoi, A., Regmi, K.R., Khadka, D.R., and Fujiwara Y., 2000, Magnetic minerals and magnetic properties of the Siwalik Group sediments of the Karnali River section in Nepal. Earth Planets Space, v. 52, p. 337-345.

Ghosh, P., Padia, J.T., and Mohindra, R., 2004. Stable isotopic studies of palaeosol sediment from Upper Siwalik of Himachal Himalaya: evidence for high monsoonal intensity during late Miocene? Palaeogeography, Palaeoclimatology, Palaeoecology. V. 206, P. 103 – 114.

Gupta, A.K., Singh, R.K., Joseph, S., Thomas, E., 2004. Indian Ocean high-productivity event (10–8 Ma): linked to global cooling or to the initiation of the Indian monsoons? Geology 32, 753–756.

Gupta, A.K., 2010. Evolution of the Indian monsoon since Late Miocene intensification: Marine and land proxy records. Journal of the palaeontological society of India. v. 55. p. 1-9.

Gupta, A.K., Yuvaraja, A., Prakasam, M., Clemens, S.C., Velu, A., 2015. Evolution of the South Asian monsoon wind system since the late Middle Miocene. Palaeogeography, Palaeoclimatology, Palaeoecology. v.438, p. 160-167.

Hagen, T., 1969. Report on the Geological Survey of Nepal (preliminary reconnaissance). Denkschr. Schweiz. naturf. Gesell. v. 86 (1), p. 1–185.

Hodges, K.v., and Silverberg, D.S., 1988. Thermal evolution of the Greater Himalaya, Garhwal, India: Tectonics, v.7. p. 583-600.

Hodges, K.V., Parrish, R.R., and Searle, M.P., 1996. Tectonic evolution of the central Annapurna range, nepalsese Himalay: Tectonics. v.15, p. 1264-1291.

Hodges, K. V., 2000. Tectonics of the Himalaya and southern Tibet from two prospective. GSA Bulletin. V.112; no. 3; p. 324 – 350.

Hoorn, C., Ojha, T., and Quade, J., 2000. Palynological evidence for vegetation development and climatic change in the Sub-Himalayan Zone (Neogene, Central Nepal). Palaeogeography, Palaeoclimatology, Palaeoecology v. 163; p. 133–161.

Hopmans, E. C., Weijers, J. W. H., Schefuß, E., Herfort, L., Damste, J. S. S., Schouten, S., 2004. A novel proxy for terrestrial organic matter in sediments based on branched and isoprenoid tetraether lipids. Earth and Planetary Sciences Letters, 224:107–116.

Huang, Y., Clemens, S.C., Liu, W., and Prell, W.L., 2007. Large-Scale hydrological change drove the late Miocene C_4 plant expansion in the Himalayan foreland and Arabian Peninsula. Geology, v. 35, p. 531 -534.

Huyghe, P., Galy, A., Mugnier, J.L., and France-Lanord, C., 2001. Propagation of the thrust system and erosion in the Lesser Himalaya: Geochemical and sedimentological evidences. Geology, v. 29, p. 1007 – 1010.

Huyghe, P., Mugnier, J.L., Gajurel, A.P., Delcaillau, B., 2005. Tectonic and climatic control of the changes in the sedimentary record of the Karnali River section (Siwaliks of Western Nepal). The Island Arc, v. 14, p. 311-327.

IAEA, 2003. GNIP/ISOHIS, Isotope Hydrology Information System of International Atomic Energy Agency. IAEA, Vienna, Austria. URL: http://isohis.iaea.org.

Khanal, S., Robinson, D.M., 2013. Upper crustal shortening and forward modeling of the Himalayan thrust belt along the Budhi-Gandaki River, central Nepal. Int J Earth Sci 102(7):1871–1891.

Konomatsu, M., 1997. Miocene leaf-fossil assemblages of the Churia (Siwalik) group of Nepal and their paleoclimate implication. Jour. Geol. Soc. Japan, 103, No. 3, p. 265-274.

Kuppusamy M., and Ghosh P., 2012. Cenozoic climate record for monsoonal rainfall over the Indian region, Modern climatology, Dr Shih-Yu Wang (Ed.), ISBN: 978-953-51-0095-9, InTech

Liu, W., Huang, Y., An, Z., Clemens, S. C., Li, L., Prell, W. L., and Ning, Y., 2005. Summer monsoon intensity controls C4/C3 plant abundance during the last 35 ka in the Chinese Loess Plateau: Carbon isotope evidence from bulk organic matter and individual leaf waxes. Science direct; Palaeogeography, Palaeoclimatology, Palaeoecology v. 220, p. 243 – 254.

Martin, J.A., DeCelles, P.G., Gehrels, G.E., Patchett, P.J., and Isachsen, C., 2005. Isotopic and structural constraints on the location of the Main Central thrust in the Annapurna Range, central Nepal Himalaya. GSA Bulletin, v. 117, p. 926-944.

Nakayama, K. and Ulak, P. D., 1999. Evolution of the fluvial style in the Siwalik Group in the foothills of Nepal Himalaya. Sediment. Geol., v. 125, p. 205–224.

Ojha T.P., Butler, R.F., DeCelles P.G., and Quade, J., 2009. Magnetic polarity stratigraphy of the Neogene foreland basin deposits of Nepal. Basin Research, v. 21, p. 61-90.

Ojha, T. P., Butler, R. F., Quade, J., DeCelles, P. G., Richards, D., and Upreti, B. N., 2000. Magnetic polarity stratigraphy of the Neogene Siwalik Group at Khutia Khola, far western Nepal. GSA Bulletin, v. 112, p. 424–434.

Peterse, F., Meer, Jaap van der., Schouten, S., Weijers, J.W.H., Fierer, N., Jackson, R.B., Kim, Jung-Hyun., Sinninghe, J.S., Damste, S., 2012. Revised calibration of the MBT–CBT paleotemperature proxy based on branched tetraether membrane lipids in surface soils. Geochim. Cosmochim. Acta, v. 96, p. 215-229.

Polissar, P.J., Freeman, K.H., Rowley, D.B., McInerney, F.A., and Currie, B.S., 2009. Paleoaltimetry of the Tibetan Plateau from D/H ratio of lipid biomarkers. Earth and Planetary Science Letter, v. 287, p. 64 – 76.

Prakash, B., Sharma, R.P, and Roy, A.K., 1980, The Siwalik Group (molasse), - sediments shed by collision of continental plates. Sediment. Geol., v. 25, p. 127-159.

Prell, L. W., Kutzbach, E. J., 1992. Sensitivity of the Indian monsoon to forcing parameters and implications for its evolution. Nature. v. 360. p. 647- 651

Quade, J., Cerling, T.E., Bowman, J.R., 1989. Development of Asianmonsoon revealed by marked ecological shift during the latest Miocene in northern Pakistan. Nature v. 342, p. 163–166.

Quade, J., Cater, J.M.L., Ojha, T.P., Adam, J., and Harrison T.M., 1995. Late Miocene environmental change in Nepal and northern Indian subcontinent: stable isotope evidence form Paleosols. GSA bulletin. V. 107; no. 12; p. 1381 – 1397.

Quade, J., and Cerling, T.E., 1995. Expansion of C_4 grasses in the Late Miocene of Northern Pakistan: evidence from stable isotope in paleosols. Palaeogeography, Palaeoclimatology, Palaeoecology v. 115, p. 91 – 116.

Quade, J., Eiler, J., Daeron, M., Achyuthan., 2013. The clumped isotope geothermometer in soil and paleosol carbonate. Geochimica et Cosmochimic Acta, v. 105; p. 92 – 107.

Raiverman, V., 2002. Foreland Sedimentation in Himalayan Tectonic Regime: A Relook at the Orogenic Process. Bishen Singh Mahendra Pal Singh, Dehra Dun, India, 378p.

Rao, R. A., Agrawal, R. P., Sharma, U. N., Bhalla, M. S., Nanda, A. C. 1988. Magnetic polarity stratigraphy and vertebrate palaeontology of the Upper Siwalik Subgroup of Jammu Hills, India. Journal of the Geological Society of India 31, 361–85.

Rowley, D. 1996. Age of initiation of collision between India and Asia: a review of stratigraphic data. Earth Planet. Sci. Lett. 145:1–13.

Ruddiman, W.F., and Kutzbach, J.E., 1989. Forcing of Late Cenozoic Northern Hemisphere Climate by plateau uplift in Southern Asia and the American West. Journal of Geophysical research. v. 95, p. 18,409-18,427.

Sachse, D., Billault, I., Gowen, G.J., Chikaraishi, Y., Dawson, T.E., Feakins, S.J., Freeman, K.H., Magill, C.R., McInerney, F.A., Meer, F.T.J., Polissar, P., Robins, R.J., Sachs, J.P., Schmidt, H.L., Sessions, A.L., White, J.W.D., West, J.B., and Kahmen, A., 2012. Molecular Paleohydrology: Interpreting the Hydrogen-Isotopic Composition of Lipid Biomarkers fromPhotosynthesizing Organisms. Annual Review. Earth Platet. Sci v. 40. P. 211 – 249.

Sanyal, P., Bhattacharya, S.K., Kumar, R., Ghosh, S.K., Sangode, S.J., 2004. Mio-Pliocene monsoonal record from Himalayan Foreland basin (Indian Siwalik) and its relation to the vegetational change. Palaeogeography, Palaeoclimatology, Palaeoecology, v. 205, p. 23–41.

Sanyal, P., Bhattachayra, S.K., and Prasad, M., 2005. Chemical diagenesis of Siwalik sandstone: Isotopic and mineralogical proxies form Surai Khola section, Nepal. Sedimentary Geology. v. 180, p. 57-74.

Sanyal, P., Sarker, A., Bhattacharya, S.K., Kumar, R., Ghosh, S.K., Agrawal, S., 2010. Intensification of monsoon, microclimate and asynchronous C4 appearance: Isotopic evidence from the Indian Siwalik sediments. Palaeogeography, Palaeoclimatology, Palaeoecology v. 228, p. 245-259.

Sangode, S.J., Kumar, R., 2003. Magnetostratigraphic correlation of the Late Cenozoic fluvial sequences from NW Himalaya. Curr. Sci. 84, 1014–1024.

Schelling, d., Carter, J., Seago, R. and Ojha, T.P., 1991: A balanced cross-section across the central Nepal Siwalik Hills: Hetauda to Amlekhganj. T.Fac. Sci., Hokkaido University, Ser. IV, 23, 19.

Schimmelmann, A., Lewan, M.D., Wintsch, R.P., 1999. D/H isotope ratios of kerogen, bitumen, oil, and water in hydrous pyrolysis of source rocks containing kerogen types I, II, and III. Geochimica et Cosmochimica Acta 63, 3751–3766.

Schott, F.A., McCreary, J.P. Jr. 2001. The monsoon circulation of the Indian Ocean. Progress in Oceanography, v. 51, p. 1-123.

Sessions AL, Sylva SP, Summons RE, Hayes JM. 2004. Isotopic exchange of carbon-bound hydrogen over geologic timescales. Geochim. Cosmochim. Acta v. 68, p.1545–59.

Singh, S., Prakash, B., Awasthi, A.K., and Singh, T., 2012. Palaeoprecipitation record using O-isotope studies of the Himalayan Foreland Basin sediments, NW India. Palaeogeography, Palaeoclimatology, Palaeoecology v. 331-332, p. 39 – 49.

Sorkhabi, R. B., Stump, E., Foland, K. A., and Jain, A. K., 1996, Fission-track and 40Ar/39Ar evidence for episodic denudation of the Gangotri granites in the Garhwal Higher Himalaya, India, Tectonophysics, 260, 187 – 199, doi:10.1016/0040-1951(96)00083-2

Stromberg, C.A.E., 2011. Evolution of Grasses and Grassland Ecosystems. Annu. Rev. Earth Planet. Sci., v. 39, p. 517–44.

Tierney, J.E., 2012. GDGT thermometry: Lipid tools for reconstructing paelotemperatures. The paleontological society paper. v. 18, p. 115 – 131.

Tipple, B. J., and Pagani, M., 2007. The Early Origins of Terrestrial C_4 Photosynthesis. Annual Review Earth Planet. Sci., v. 35, p. 435-61.

Tipple, B.J., and Pagani, M., 2010. A 35 Myr North American leaf-wax compound-specific carbon and hydrogen isotope record: Implications for C4 grasslands and hydrologic cycle dynamics. Science Direct, Earth and Planetary science letters v. 299; p. 250 – 262.

Tokuoka, T., Takayasu, K., Yoshida, M. and Hisatomi, K., 1986. The Churia (Siwalik) Group of Arungg Khola area, west-central Nepal. Mem. Fac. Sci. Shimane Univ., v. 22, p. 135-210.

Ulak, P.D., 2009. Lithostratigraphy and late Cenozoic fluvial styles of Siwalik Group along Kankai River section, East Nepal Himalaya. Bulletin of the Department of Geology, Tribhuvan University, Kathmandu, Nepal. v. 12, p. 63-74.

Upreti B (1999) An overview of the stratigraphy and tectonics of the Nepal Himalaya. J Asian Earth Sci 17(5):577–606

Urban, M.A., Nelson, D.M., Moreno. G.J., Châteauneuf, J.J., Pearson, A., and Hu, F.S., 2010. Isotopic evidence of C4 grasses in southwestern Europe during the Early Oligocene–Middle Miocene. Geology, GSA v. 38; no. 12; p. 1091 – 1094.

Weijers J. W. H., Schouten S., van den Donker J. C., Hopmans E.C. and Sinninghe Damste´ J. S., 2007. Environmental controls on bacterial tetraether membrane lipid distribution in soils. Geochim. Cosmochim. Acta 71, 703–713.

Yoshida, M. and Arita, K., 1982, On the Siwaliks observed along some routes in Central Nepal. Jour. Nepal. Geol. Soc., v. 2, Spec. Issue, p. 51-58.

VITA

Prabhat Chandra Neupane was born in Nepal, the country of the Himalayas on April 14th 1979. He is the youngest son among his four brothers. He started his educational journey at the age of 5. From the childhood he was nature lover and was highly fascinated by the meandering rivers, snowcapped mountains and high elevated hills close to his home. During the high school studies, he trekked numerous mountainous places and experienced the unique topographic terrains, orientation of rocks and colorful minerals up close. To decipher the mystery of nature, he took geology as a major during his B.Sc. studies at Tri-Chandra Campus, Tribhuvan University, Nepal. He continued his M.Sc. at Central Department of Geology, Tribhuvan University and graduated in 2004. After his graduation, he started his professional carrier in Nepal for four years involving as a consultant geologist in different mining companies and also worked as a freelance geologist. During his job, he got many opportunities to get involved in different geological researches conducted by national and international institutions in the Nepalese Himalaya. His interaction with various national and international scholars provided him with a new vision and desire for the higher studies at United States. To fulfill his goals and objectives, he joined the Department of Earth and Environmental Sciences, University of New Orleans, Louisianan in 2010 (spring) as a graduate (MS) student and completed his master's degree in December 2011. To continue his further education, he again enrolled as a PhD student at the same university from spring 2012 and successfully completed his PhD in May 2017.